

# STRUCTURE AND ENVIRONMENT

KIELCE UNIVERSITY OF TECHNOLOGY

Quarterly  
Vol. 16, No. 3, 2024

ISSN 2081-1500  
e-ISSN 2657-6902

• Architecture and urban planning • Civil engineering and transport • Environmental engineering, mining and energy



Available online at: <https://sae.tu.kielce.pl>

# Contents

## structure structure

---

MAJA KĘPNIAK, JUSTYNA PSKOWSKA, ALEKSANDRA GARUS, MICHAŁ DRABCZYK, SEBASTIAN KASPER <b>THE IMPACT OF RECYCLED FINE AGGREGATE ON SELECTED PROPERTIES OF CONCRETE</b> WPŁYW DROBNEGO KRUSZYWA Z RECYKLINGU NA WYBRANE WŁAŚCIWOŚCI BETONU .....	129
MICHAŁ ŁACH, AGNIESZKA PRZYBEK, KINGA SETLAK, PATRYCJA BAZAN, MARIA HEBDOWSKA-KRUPA <b>RESISTANCE OF LOW-EMISSION GEOPOLYMER BINDERS WITH FIBERS TO AGGRESSIVE EXTERNAL FACTORS</b> ODPORNOŚĆ NISKOEMISYJNYCH SPOIW GEOPOLIMEROWYCH Z WŁÓKNAMI NA DZIAŁANIE AGRESYWNYCH CZYNNIKÓW ZEWNĘTRZNYCH .....	134
MAREK IWAŃSKI, GRZEGORZ MAZUREK, PRZEMYSŁAW BUCZYŃSKI <b>ANALYSIS OF THE DEFORMATION OF ROAD SURFACE CONSTRUCTION BASED ON MONITORING CLIMATIC FACTORS</b> ANALIZA ODKształceń KONSTRUKCJI NAWIERZCHNI DROGI NA PODSTAWIE MONITORINGU CZYNNIKÓW KLIMATYCZNYCH .....	141
KALINA MATERAK, ALICJA WIECZOREK, MARCIN ZASADA, MARCIN KONIORCZYK <b>THE IMPACT OF INTERNAL HYDROPHOBIZATION ON THE PROPERTIES OF THE CEMENT-BASED MATERIALS WITH MINERAL ADDITIVES</b> WPŁYW HYDROFOBIZACJI OBJĘTOŚCIOWEJ NA WŁAŚCIWOŚCI MATERIAŁÓW CEMENTOWYCH Z DODATKAMI MINERALNYMI .....	148
KINGA DZIEDZIC, MICHAŁ A. GLINICKI <b>ASSESSMENT OF AGGREGATE MIXTURE REACTIVITY IN CONCRETE AT 60 °C</b> OCENA REAKTYWNOŚCI MIESZANINY KRUSZYW W BETONIE W TEMPERATURZE 60 °C .....	153
ZOFIA SZWEDA <b>THE INFLUENCE OF CHLORIDE IONS CONTENT ON THE MECHANICAL PROPERTIES OF CONCRETE</b> WPŁYW ZAWARTOŚCI JONÓW CHLORKOWYCH NA WŁAŚCIWOŚCI MECHANICZNE BETONU .....	158
JUSTYNA ZAPAŁA-SŁAWETA, KAMIL ZIĘBA <b>A NEW APPROACH TO THE ACCELERATED METHOD FOR ASSESSING THE ALKALI REACTIVITY OF DOMESTIC AGGREGATES</b> NOWE PODEJŚCIE DO PRZYSPIESZONEJ METODY BADANIA REAKTYWNOŚCI ALKALICZNEJ KRUSZYW KRAJOWYCH .....	166
<b>ABSTRACTS</b> .....	175

**Editor-in-Chief:**

Zdzisława OWSIAK, Kielce University of Technology, Poland

**Managing Editor:**

Justyna ZAPŁA-SŁAWETA, Kielce University of Technology, Poland

**Editorial Advisory Board:**

Joanna GIL-MASTALERCZYK, Kielce University of Technology, Poland

Agata JANASZEK, Kielce University of Technology, Poland

Grzegorz MAZUREK, Kielce University of Technology, Poland

**Editors:**

Vadim ABIZOV, Kyiv National University of Technologies and Design, Ukraine

Satoshi AKAGAWA, Hokkaido University, Sapporo, Japan

Tomasz ARCISZEWSKI, George Mason University, USA

Łukasz BAŁ, Kielce University of Technology, Poland

Mark BOMBERG, McMaster University, Canada

Jan BUJNAK, University of Žilina, Slovakia

Adela Perez GALVIN, University of Cordoba, Portugal

Go IWAHANA, University of Alaska Fairbanks, USA

Marek IWAŃSKI, Kielce University of Technology, Poland

Andrej KAPJOR, University of Žilina, Slovakia

Tomasz KOZŁOWSKI, Kielce University of Technology, Poland

Jozef MELCER, University of Žilina, Slovakia

Mikhail NEMCHINOV, Moscow State Automobile and Road Technical University MADI, Russia

Andrzej S. NOWAK, Auburn University, USA

Jerzy Z. PIOTROWSKI, Kielce University of Technology, Poland

Karel POSPÍŠIL, The Transport Research Centre CDV, Czech Republic

Claude van ROOTEN, Belgian Road Research Centre, Belgium

Milan SOKOL, Slovak University of Technology in Bratislava, Slovakia

Grzegorz ŚWIT, Kielce University of Technology, Poland

Jerzy WAWRZEŃCZYK, Kielce University of Technology, Poland

Janusz WOJTKOWIAK, Poznan University of Technology, Poland

Piotr WOYCIECHOWSKI, Warsaw University of Technology, Poland

**Language Editors:**

Łukasz ORMAN, Kielce University of Technology, Poland

**Technical Editors:**

Marek BIAŁEK, Kielce University of Technology, Poland

Tadeusz UBERMAN, Kielce University of Technology, Poland

**Cover design:**

Waldemar KOZUB, Kielce University of Technology, Poland

**General data:**

Format of the journal – electronic form

Frequency of publication – quarterly

The quarterly issues of Structure and Environment are their original versions

e-ISSN 2657-6902

ISSN 2081-1500

DOI: 10.30540/sae/0000

**The journal published by:**

Kielce University of Technology, Tysiąclecia Państwa Polskiego 7 Str. 25-314 Kielce, Poland

T.: +48 41 342 45 41

De Gruyter Poland:

Bogumiła Zuga 32A Str. 01-811 Warsaw, Poland

T.: +48 22 701 50 15

**Journal Metrics:**

Index Copernicus Value (IVC) 2023 = 100

The Polish Ministry of Education and Science 2024 = 40 points



**Kielce University of Technology**  
2024

INDEX  COPERNICUS  
I N T E R N A T I O N A L



**structure**  
structure



# THE IMPACT OF RECYCLED FINE AGGREGATE ON SELECTED PROPERTIES OF CONCRETE

## WPŁYW DROBNEGO KRUSZYWA Z RECYKLINGU NA WYBRANE WŁAŚCIWOŚCI BETONU

Maja Kępnia\*, Justyna Pskowska, Aleksandra Garus  
Warsaw University of Technology, Poland  
Michał Drabczyk, Sebastian Kasper  
Holcim Polska S.A.

### Abstract

*The use of recycled fine aggregate in the production of concrete mixes is one of the elements of a circular economy. However, it is important to ensure that such a modification does not significantly affect the durability of the produced concrete elements. One possible criterion to check whether this condition is met is the practical application of the concept of equivalent concrete properties. The presented studies analyzed the properties of concrete with multi-component cement CEM V/A (S-V) and with recycled fine aggregate. The conducted analyses of the research results showed that with a 15% replacement level of natural sand with recycled sand, it is possible to maintain durability characteristics compared to concrete using only natural sand.*

**Keywords:** fine recycled aggregate, concrete durability, equivalent characteristics

### Streszczenie

*Stosowanie drobnego kruszywa z recyklingu do produkcji mieszanek betonowych jest jednym z elementów gospodarki w obiegu zamkniętym. Należy jednak zwrócić uwagę, aby taka modyfikacja nie wpłynęła znacząco na trwałość wykonywanych elementów betonowych. Jednym z możliwych kryteriów jest sprawdzenie, czy warunek ten jest spełniony, jest zastosowanie w praktyce koncepcji równoważnych właściwości betonu. W przedstawionych badaniach analizowano właściwości betonu z cementem wieloskładnikowym CEM V/A (S-V) oraz z drobnym kruszywem z recyklingu. Przeprowadzone analizy wyników badań wykazały, że przy 15% stopniu zastąpienia piasku naturalnego piaskiem z recyklingu możliwe jest zachowanie cech związanych z trwałością w stosunku do betonu z użyciem wyłącznie piasku naturalnego.*

**Słowa kluczowe:** drobne kruszywo z recyklingu, trwałość betonu, cechy równoważne

### 1. INTRODUCTION

Currently, many directives and regulations, as well as numerous scientific studies, focus on the carbon footprint [1, 2]. However, increasing attention is being directed towards the circular economy, including the management of the numerous wastes generated from construction and demolition activities

[3-5]. Eco-friendly solutions, apart from meeting the goals of the lowest possible carbon footprint and waste management, should ensure the appropriate durability of concrete and the entire structure [6, 7]. The current PN-EN 206 standard partially limits the qualitative or quantitative use of certain eco-friendly solutions, such as the substitution of natural aggregate

\*Warsaw University of Technology, Poland, e-mail: [maja.kepnia@pw.edu.pl](mailto:maja.kepnia@pw.edu.pl)

with recycled aggregate in more demanding exposure classes. However, the standard allows for the use of such solutions provided that equivalent performance characteristics are ensured. A beneficial solution, particularly for multi-component cements with low clinker content, is the equivalent test time for non-strength-related tests as included in the national supplement PN-B-06265 to the PN-EN 206 standard. Durability-related characteristics can be verified after a longer period than the standard 28 days, i.e., after 56 or 90 days of curing. A similar relationship is also noticeable when using type II additives, as well as when using type I additives in the form of fine-grained waste materials [8, 9].

The use of fine recycled aggregate is the subject of numerous scientific studies [10, 11]. Mortars modified with fine recycled aggregate can exhibit comparable or even better strength and durability characteristics than those with natural aggregate [12, 13]. The use of processed fine-grained material from crushed aerated concrete elements or ceramic bricks has been found to increase the strength of the mortar and contribute to more effective microstructure sealing, consequently improving durability [12]. Recycled sand is also used as a component in self-compacting concrete mixtures, positively influencing both the rheological and durability properties of this type of concrete [14, 15]. Ensuring durability in many co-existing exposure classes is a complex problem, especially when using concrete mixtures that simultaneously have a reduced carbon footprint and contain waste materials. Therefore, such mixtures should always be considered multi-critically to ensure the appropriate durability of concrete elements while minimizing environmental impact throughout the entire life cycle of the building [16]. The presented studies analyzed the durability-related characteristics, carbonation, and chloride ion migration of low-carbon concrete with fine recycled aggregate from construction debris.

## 2. MATERIALS AND METHODS

The studies designed five concrete mixtures differing in the level of replacement of natural sand with fine recycled aggregate (FRA), ranging from 0% to 60%. The concrete mix design specifications included: strength class C30/37, consistency class S3 or S4, a maximum aggregate size of 16 mm, and exposure classes: XD1 and XC4. The qualitative selection of concrete mix components included: multi-component cement CEM V/A (S-V) with a strength class of 42.5 N (28-day strength according to PN-EN 196-1 is

58.1 MPa, and 2-day strength is 20.0 MPa) and a net carbon footprint of 323 kg/t, fly ash, gravel aggregate 2/16, crushed dolomite aggregate 8/16, river sand 0/2, and local recycled sand from construction debris (gradation – Fig. 1).

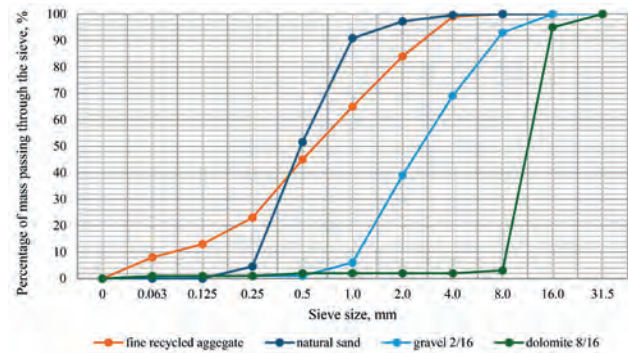


Fig. 1. Aggregate grading

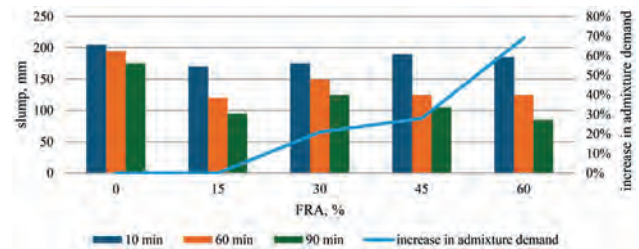


Fig. 2. Changes in consistency over time depending on the proportion of fine recycled aggregate (FRA)

The apparent density of recycled sand grains was 2.59 g/cm<sup>3</sup>, and its water absorption was 8.2%. The apparent density of natural sand grains was 2.64 g/cm<sup>3</sup>. Two admixtures from the water-reducing group were used: a plasticizing admixture containing lignosulfonate and gluconate, and a superplasticizing admixture containing modified polycarboxylate ether (PCE) dosed to achieve the desired consistency (Table 1, Fig. 2). The effective water-to-cement ratio was constant for all mixtures and was 0.54.

The preparation of concrete mixes also required the use of a composition of water-reducing admixtures, dosed in varying amounts to achieve the desired consistency. As the proportion of recycled sand increased, it became necessary to increase the dosage of admixtures to obtain a slump of approximately 200 mm. However, maintaining consistency over time was problematic. This was likely due to the significant water demand of the recycled aggregate, as it absorbed water from the concrete mix, resulting in a significant reduction in slump, by as much as two classes, with higher amounts of added recycled aggregate.

Table 1. Compositions per 1 m<sup>3</sup> of analyzed concrete mixtures depending on the proportion of fine recycled aggregate (FRA)

FRA content in sand mass	0%	15%	30%	45%	60%
CEM V/A(S-V), kg	300	300	300	300	300
Fly ash, kg	50	50	50	50	50
Effective water, kg	163	163	163	163	163
Natural sand 0/2, kg	765	641	516	392	285
Fine recycled aggregate, kg	0	114	228	341	439
Gravel 2/16, kg	751	751	751	751	751
Dolomite 8/16, kg	280	280	280	280	280
Plasticizing admixture, kg	1.35	1.35	1.35	1.35	1.35
Superplasticizing admixture, kg	0.946	0.946	1.146	1.200	1.600

The study determined the compressive strength of concrete according to PN-EN 123903, water penetration under pressure according to PN-EN 12390-8, chloride ion migration according to PN-EN 12390-18, and carbonation according to PN-EN 12390-12.

### 3. RESULTS

The compressive strength of the analyzed concretes was tested at two intervals: after 28 and 56 days (Fig. 3). It was observed that the qualitative change and addition of 15% recycled sand minimally affect compressive strength, especially when analyzing strength after 56 days, which is justified by the use of CEM V/A(S-V) cement. Above the threshold of 30% recycled aggregate content, there is a deterioration in compressive strength, with the difference between strength after 28 days and after 56 days being smaller compared to lower percentages of recycled aggregate. It should be noted that even at the maximum analyzed content of fine recycled aggregate, the achieved compressive strength meets the requirements of class C30/37 after 56 days of curing.

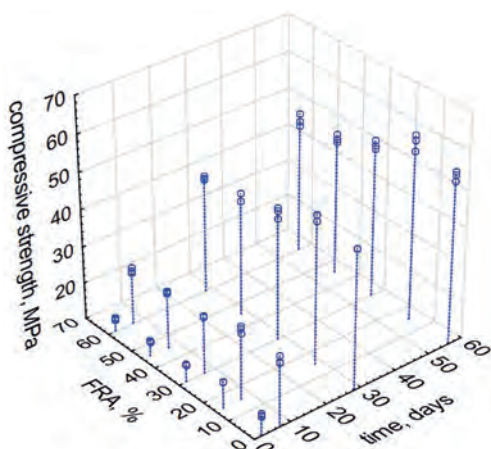


Fig. 3. Development of compressive strength over time depending on the degree of substitution of natural fine aggregate with recycled fine aggregate (FRA)

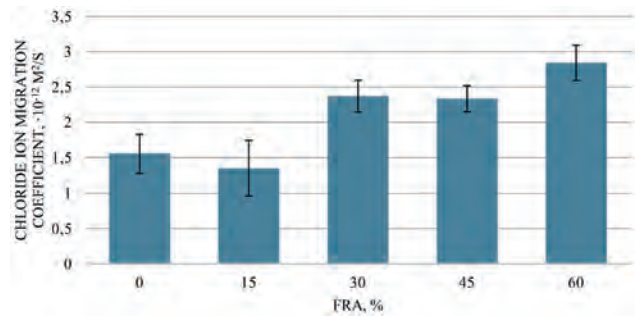


Fig. 4. Chloride ion migration coefficient depending on the degree of substitution of natural fine aggregate with recycled fine aggregate

The chloride ion migration coefficient of the reference composition (without fine recycled aggregate) and the composition with 15% recycled sand differed by less than the standard deviations of the results and were very low, indicating excellent impermeability and resistance to chloride ion penetration. Mixtures with higher proportions of recycled sand had higher chloride ion migration coefficients, ranging from 2.3 to 2.8 × 10<sup>-12</sup> m<sup>2</sup>/s on average, which also indicate good resistance to chloride ion penetration (Fig. 4). The chloride ion migration coefficient can be interpreted as very good below 2 × 10<sup>-12</sup> m<sup>2</sup>/s and as good below 8 × 10<sup>-12</sup> m<sup>2</sup>/s [17].

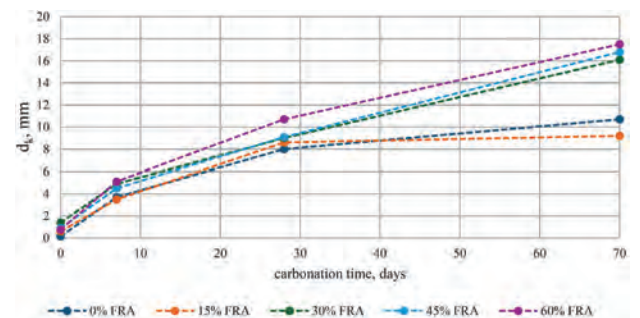


Fig. 5. Depth of carbonation over time depending on the degree of substitution of natural fine aggregate with recycled fine aggregate





The shape and slope characteristics of the depth of carbonation curve over time reflect the susceptibility of concrete to the carbonation process – the steeper the slope, the greater the susceptibility to this process (Fig. 5). It is worth noting that the higher the content of recycled aggregate, the steeper the curve, and the average depth of carbonation increases. This indicates that concrete containing more than 15% by weight of recycled sand has less resistance to carbonation. The curves for compositions containing 30%, 45%, and 60% recycled aggregate respectively resemble a linear function, suggesting that over time,

they may become less resistant to the negative effects of carbonation. In contrast, the depth of carbonation for reference samples and those containing 15% fine recycled aggregate shows a slight increase after 30 days (Fig. 5).

The depth of water penetration under pressure can also be considered as a measure of durability (impermeability). The depth of water penetration under pressure increased with an increased proportion of recycled sand. However, for none of the analyzed concretes did it exceed 30 mm, indicating good water tightness of the concrete.
































#### 4. CONCLUSIONS AND SUMMARY

Due to the fact that the results of durability characteristics are not straightforward, they have been compiled in tabular form (Table 2) for comparison purposes. This arrangement facilitates comparing the properties of concretes with varying amounts of recycled aggregate relative to the reference composition, which serves as a benchmark. Single

upward arrows  indicate a slight increase in the value of a parameter, while double upward arrows  indicate a noticeable increase. Conversely, downward arrows  indicate a slight decrease, while  indicate a significant decrease. Arrows on a red background signify worse results in the study compared to the reference sample, whereas green arrows indicate improved properties.

In summary of the presented research results, it can be concluded that substituting natural fine aggregate with recycled fine aggregate at a level of 15% allows achieving durability properties at least equivalent to those of the reference concrete. Therefore, despite the limitation in the dosage of fine recycled aggregate, using it up to 15% can still maintain comparable concrete characteristics. This approach is beneficial due to environmental advantages such as conservation of natural resources. However, it is essential to consider the variability in properties of recycled fine aggregate depending on its origin and processing method.

Table 2. Comparative summary of research results depending on the level of substitution of natural fine aggregate with recycled fine aggregate (FRA)

	Consistency		Compressive strength		Carbonation		Penetration	Chloride ion migration
	Admixture [% c.m.]	Consistency retention [mm]	[MPa]	[MPa]	Depth $d_k$ [mm]	Rate. $K_{AC}$ [mm/ $\sqrt{\text{dni}}$ ]	Depth under pressure [mm]	The chloride ion migration coefficient [ $\cdot$ [m <sup>2</sup> /s]]
Test time	0 min	90 min	28 days	56 days	70 days	70 days	90 days	90 days
FRA 0%	0.77	30	48.0	55.4	10.7	1.29	4	1.56
FRA 15%	–							
FRA 30%								
FRA 45%								
FRA 60%								

#### REFERENCES

- [1] Jacobsen Ø.E.K., Kristoffersen M., Dey S., Børvik T., *Sustainable shielding: Ballistic performance of low-carbon concrete*, Constr. Build. Mater., vol. 415, 2024, doi: 10.1016/j.conbuildmat.2024.135103.
- [2] Nazari A., Sanjayan J.G.B.T.-H. of L.C.C., Eds., “Copyright”, Butterworth-Heinemann, 2017, p. iv. doi: <https://doi.org/10.1016/B978-0-12-804524-4.00017-8>.
- [3] Shmls M., Abed M., Fořt J., Horvath T., Bozsaky D., *Towards closed-loop concrete recycling: Life cycle assessment and multi-criteria analysis*, J. Clean. Prod., vol. 410, p. 137179, 2023, doi: <https://doi.org/10.1016/j.jclepro.2023.137179>.
- [4] Habibi A., Bamshad O., Golzary A., Buswell R., Osmani M., *Biases in life cycle assessment of circular concrete*, Renew. Sustain. Energy Rev., vol. 192, p. 114237, 2024, doi: <https://doi.org/10.1016/j.rser.2023.114237>.



- [5] De Schepper M., Van den Heede P., Van Driessche I., De Belie N., *Life Cycle Assessment of Completely Recyclable Concrete*, *Materials*, vol. 7, no. 8. pp. 6010–6027, 2014. doi: 10.3390/ma7086010.
- [6] Maj M., Grzymiski F., Ubysz A., *The loss of durability in reinforced concrete structures*, *J. Phys. Conf. Ser.*, vol. 1425, no. 1, p. 12207, 2019, doi: 10.1088/1742-6596/1425/1/012207.
- [7] Chemrouk M., *The Deteriorations of Reinforced Concrete and the Option of High Performances Reinforced Concrete*, *Procedia Eng.*, vol. 125, pp. 713–724, 2015, doi: <https://doi.org/10.1016/j.proeng.2015.11.112>.
- [8] Kępnia M., Woyciechowski P., *Influence of sand substitution with waste lime powder on the concrete carbonation*, *Arch. Civ. Eng.*, vol. 67, no. No 4, pp. 383–392, 2021, doi: 10.24425/ace.2021.138506.
- [9] Dobiszewska M., Kuziak J., Woyciechowski P., Kępnia M., *Główne aspekty trwałości betonu modyfikowanego odpadowym pyłem bazaltowym z odpylania kruszyw w wytwórni MMA*, *J. Civ. Eng. Environ. Archit.*, 2016, doi: 10.7862/rb.2016.13.
- [10] El Abidine Tahar Z., Kadri E.H., Benabed B., Ngo T.-T., *Influence of cement type and chemical admixtures on the durability of recycled concrete aggregates*, *Mag. Civ. Eng.*, vol. 109, no. 1, 2022, doi: 10.34910/MCE.109.8.
- [11] Guo M., Gong G., Yue Y., Xing F., Zhou Y., Hu B., *Performance evaluation of recycled aggregate concrete incorporating limestone calcined clay cement (LC3)*, *J. Clean. Prod.*, vol. 366, p. 132820, 2022, doi: <https://doi.org/10.1016/j.jclepro.2022.132820>.
- [12] Liu Q., Singh A., Xiao J., Li B., Tam V.W.Y., *Workability and mechanical properties of mortar containing recycled sand from aerated concrete blocks and sintered clay bricks*, *Resour. Conserv. Recycl.*, vol. 157, p. 104728, 2020, doi: <https://doi.org/10.1016/j.resconrec.2020.104728>.
- [13] Le M.T., Tribout C., Escadeillas G., *Durability of mortars with leftover recycled sand*, *Constr. Build. Mater.*, vol. 215, pp. 391–400, 2019, doi: <https://doi.org/10.1016/j.conbuildmat.2019.04.179>.
- [14] Hadidi M.R. Mohammadi Y., *The effect of the freeze-thaw cycle and alkali-silica reaction on self-compacting recycled concrete*, *Eur. J. Environ. Civ. Eng.*, 2024, [Online]. Available: <https://api.semanticscholar.org/CorpusID:268354187>.
- [15] Sujatha T.S., Murty D.V.R., *Experimental Investigation on Durability Study of Portland Slag Concrete with Influence of High-Volume Recycled Aggregate*, *Civ. Eng. Archit.*, 2023, [Online]. Available: <https://api.semanticscholar.org/CorpusID:258047943>.
- [16] Kępnia M., Łukowski P., *Multicriteria Analysis of Cement Mortar with Recycled Sand*, *Sustainability*, vol. 16, no. 5. 2024. doi: 10.3390/su16051773.
- [17] Tang L., *Concentration dependence of diffusion and migration of chloride ions: Part 1. Theoretical considerations*, *Cem. Concr. Res.*, vol. 29, no. 9, pp. 1463–1468, 1999, doi: [https://doi.org/10.1016/S0008-8846\(99\)00121-0](https://doi.org/10.1016/S0008-8846(99)00121-0).



# RESISTANCE OF LOW-EMISSION GEOPOLYMER BINDERS WITH FIBERS TO AGGRESSIVE EXTERNAL FACTORS

## ODPORNOŚĆ NISKOEMISYJNYCH SPOIW GEOPOLIMEROWYCH Z WŁÓKNAMI NA DZIAŁANIE AGRESYWNYCH CZYNNIKÓW ZEWNĘTRZNYCH

Michał Łach\*, Agnieszka Przybek, Kinga Setlak, Patrycja Bazan, Maria Hebdowska-Krupa  
Cracow University of Technology, Poland

### Abstract

*Materials called geopolymers are considered an alternative to common hydraulic binders, but they have certain limitations in many applications due to their brittleness. The use of fibers to reinforce geopolymers can bring the expected results by increasing their compressive strength. This paper presents the results of accelerated durability tests of geopolymers based on coal shale and fly ash reinforced with natural fibers (1% by mass). The results of testing the resistance of such composites to UV radiation, variable temperature cycles and the results of the thermal conductivity coefficient are presented.*

**Keywords:** geopolymer, natural fiber, composite, aging test; thermal resistance, UV resistance

### Streszczenie

*Materiały zwane geopolimerami uznawane są za alternatywę dla powszechnych spoiw hydraulicznych jednak posiadają one pewne ograniczenia w wielu zastosowaniach ze względu na ich kruchość. Zastosowanie włókien do zbrojenia geopolimerów może przynieść oczekiwane rezultaty zwiększając ich wytrzymałość na zginanie. W niniejszej pracy zaprezentowano wyniki przyspieszonych badań trwałości geopolimerów na bazie łupków węglowych i popiołu lotnego wzmocnionych włóknami naturalnymi (1% mas.). Przedstawiono wyniki badań odporności takich kompozytów na działanie promieniowania UV, zmiennych cykli temperaturowych oraz przedstawiono wyniki badań współczynnika przewodzenia ciepła.*

**Słowa kluczowe:** geopolimery, włókna naturalne, kompozyty, badania starzeniowe, odporność termiczna, odporność UV

### 1. INTRODUCTION

Geopolymer composites have been known for at least several decades. One of the main motivations for researching and producing this type of material is that it is less harmful to the environment compared to materials based on hydraulic binders such as Portland cement [1, 2]. However, these materials are characterized by high

brittleness, so it is necessary to reinforce them with fibers with different properties such as high corrosion resistance, resistance to alkaline environment or high mechanical strength. Different types of fibers such as steel, polymer, basalt, carbon and also natural fibers and increasingly so-called hybrid fibers are tested [3]. Most of the scientific work is concerned with the manufacture

of geopolymer composites reinforced with synthetic fibers [4, 5], but there is a growing interest in the use of natural fibers. Detailed studies are needed in this area to evaluate the durability of such solutions and the effect of the addition of natural fibers on physical and mechanical properties. Studies conducted to date [6-10] allow us to conclude that natural fibers can successfully replace synthetic fibers in geopolymer composites.

The use of natural fibers creates a number of advantages in terms of their availability, biodegradability and diversity, but can also bring a number of limitations related to the durability of these fibers. Studies have shown that geopolymer composites containing 1% ramie, hemp and bamboo fibers and 2% ramie fibers show higher compressive and tensile strengths and lower shrinkage than unreinforced geopolymers, with those containing 1% ramie fibers showing the highest strength and lowest shrinkage [11]. Banana-derived fibers are also used [12], which can realistically improve the aging resistance of geopolymers. Tests conducted under alternating freeze-thaw cycles showed that geopolymer composites containing 1.5 wt.% banana fibers had higher cohesion and less material damage compared to unreinforced samples. As studies have shown, natural fibers added to geopolymers can also help improve insulating properties and thermal energy storage capacity, as well as improve thermal stability [13, 14].

A very important issue related to the possibility of using natural fibers in concretes is to develop a method of manufacturing and introducing these fibers in such a way that the produced composites are resistant to high temperatures. This is particularly important in foamed insulating geopolymer materials, which are characterized by good thermal conductivity values and high thermal resistance up to temperatures of the order of 1000°C [15]. The scientific literature also gives many examples related to problems with the use of natural fibers. For example, the absorbency and moisture sensitivity of natural fibers such as jute, sisal and cotton can be a problem. The addition of such fibers can increase water absorption and chloride penetration through concrete (geopolymer) [16]. In order to increase the possibility of using environmentally beneficial biodegradable and renewable natural fibers, scientific research should focus on evaluating the durability of such fibers in a geopolymer matrix [17]. This is particularly important precisely in the case of alkali-activated composites or geopolymers, where the activator concentrations used are alkaline in nature and the use of such materials in humid

environments constantly exposes the fibers present in the composite to harmful alkaline solutions. Alkalis present in geopolymers are capable of dissolving the main components of the fibers, especially lignin and hemicellulose. This can lead to a complete loss of fiber integrity especially with changes in humidity and temperature. In addition, the expansion and contraction of fibers associated with environmental changes results in the formation of tiny microcracks. This can result in complete loss of fiber strength properties and loss of long-term viability of the composites [18].

As presented in a number of scientific papers [19-25], the addition of fibers to binders may involve the need for appropriate treatment to increase their durability or improve the quality of the bond between the fibers and matrix. Cellulose is the compound responsible for the fiber's strength, while lignin and hemicellulose are responsible for its low durability, so it is often necessary to carry out treatments, most often with alkaline solutions, to improve the adhesion of the matrix to the fiber in the contact area. It has been confirmed, for example, that fibers such as açai, jute, sisal, bamboo and curaua can be used after appropriate treatment as a filler in cement matrices [26]. Kenaf fibers are also a promising addition to geopolymers due to their properties [27]. The authors of many works show that the properties of composites with fibers, in addition to their processing, can also be influenced by the way they are extracted from plants [28]. Some chemical modification of the fiber surface (e.g., the use of nano-additives) may also be recommended to improve contact at the fiber-matrix interface [29].

This paper presents the results of selected studies of geopolymer composites with natural fibers conducted to confirm the suitability of natural fibers as reinforcement of geopolymers based on specific precursors found locally in Poland. Rarely used calcined coal shale and ash from lignite combustion were used as precursors. Quantities of these precursors exist in Poland in the tens of millions of tons and their management is of great importance. The composites tested were produced by adding 1% by weight of fibers such as wood wool fibers, field grass fibers, and rafia fibers. The produced composites were subjected to flexural strength tests, accelerated aging tests in a UV chamber, tests of resistance to varying temperature cycles and determination of the thermal conductivity coefficient.

## 2. MATERIALS AND METHODS

Geopolymer composites were produced using precursors such as calcined coal slate from the heaps of the Janina Mine in Libiąż (TAURON) and lignite

combustion ash from the Bełchatów Power Plant. The microstructure of the raw materials is shown in Figure 1 and the oxide composition is presented in Table 1. Microstructure observations showed that the lime fly ash is characterized by irregular particles different from conventional fly ash from pulverized coal boilers (probably the ash contains a small amount of amorphous phase). The microstructure of calcined coal shale is similar to that of metakaolin (calcined coal shale contains about 30-40% metakaolin).

fibers of field grasses found locally in Poland (supplier Dach-Wkręt, Poland) and wood fibers (produced in the form of wood wool (supplier Dach-Wkręt, Poland)). The appearance of the fibers is shown in Figure 2. Geopolymer composites were produced with the addition of 1% fibers (short- 1-1.5 cm; long- 5-7 cm). The fibers were added to the geopolymers already after the geopolymer mass was formed and mixed for about 15 min until the composition became homogeneous.

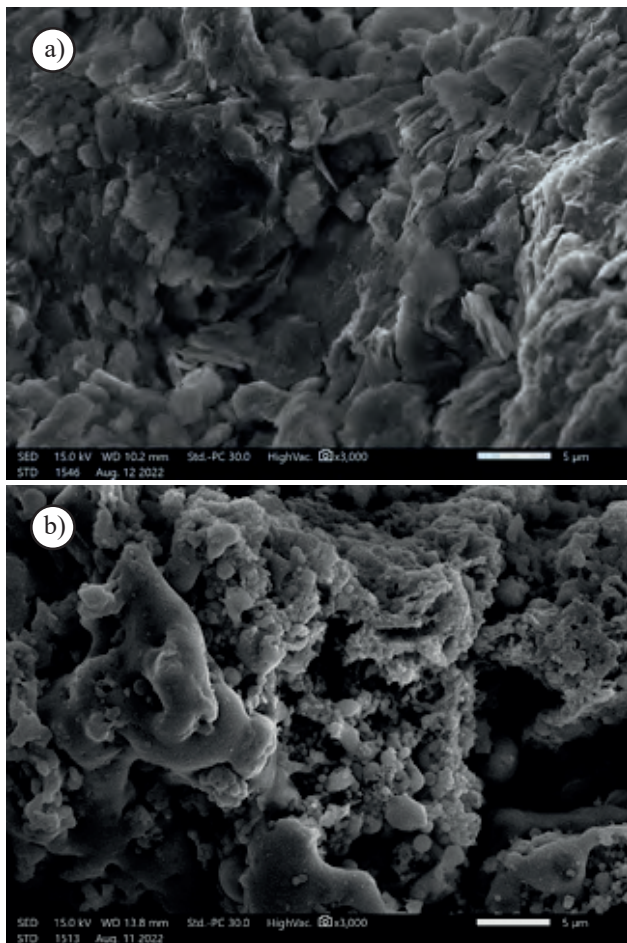


Fig. 1. Microstructure of raw materials used in the study as precursors of the geopolymerization process: a) calcined coal slate; b) lime fly ash

Table 1. Oxide composition of geopolymerization precursors used in the study

Oxide composition [wt.%]	SiO <sub>2</sub>	Al <sub>2</sub> O <sub>3</sub>	CaO	MgO	K <sub>2</sub> O	Na <sub>2</sub> O	Others
Lime fly ash	14.51	49.00	33.10	0.95	0.2	–	2.24
Calcined coal slate	55.84	36.91	0.94	1.26	3.51	0.34	1.20

The following 3 types of natural fibers were used as reinforcing fibers: rafia fibers (supplier NeoPak, Poland),



Fig. 2. Overview photo of the fibers used in the study to reinforce geopolymer materials: a) rafia; b) field grass fibers; c) wood wool fibers

Table 2. Designations of manufactured composite variants

Geopolymer \ Fibers	1% rafia – long fiber	1% rafia – short fiber	1% grass fiber-long fiber	1% grass fiber-short fiber	1% wood wool – long fiber	Reference samples
Lime fly ash	RD.B	RK.B	TD.B	TK.B	DD.B	REF.B
Calcinated coal slate	RD.Ł	RK.Ł	TD.Ł	TK.Ł	DD.Ł	REF.Ł

Geopolymers were produced using a 10M sodium hydroxide solution, with R-145 sodium glass (aqueous sodium silicate solution). The ratio of sodium hydroxide solution to water glass was 1:2.5 by weight. Geopolymers were produced using 50 parts by weight of building sand, 50 parts by weight of ash or shale, 17.5 parts by weight of alkali solution (sodium hydroxide solution + water glass). Curing was carried out at 75°C for a period of 24 hours. Table 2 shows the determinations of the geopolymer composite variants produced.

Thermal conductivity tests were carried out using NETZSCH's HFM 446 Lambda Series. The measurements were carried out for the temperature range of 0-20°C. For the tests, 16×16×5 cm panels with dimensions of 16×16×2.5 cm were prepared by cutting from the manufactured samples.

Accelerated aging tests were carried out in a Q-UV SPRAY (Q-LAB) chamber by simulating sunlight, rain and dew using alternating cycles of UV light and moisture at controlled elevated temperature. Tests were performed in accordance with ASTM G-155 [30] Cycle 7 (UV intensity 1.55 W/m<sup>2</sup>/nm; total time 500 h; spray time 0.15 h; condensation time 3.45 h, condensation temperature 50°C). Resistance tests to varying temperature cycles were carried out in a WEISS TECHNIK climate chamber for a temperature change cycle from -40°C to +40°C. The duration of one cycle was 2.5 h. The study was carried out by simulating the temperature change over 135 cycles.

Microscopic images were taken on a JEOL IT200 scanning electron microscope. Flexural strength tests were performed using an MTS Criterion testing machine according to PN-EN 12390-5:2019-08 [31].

### 3. RESULTS

Table 3 shows the results of testing the thermal conductivity coefficient of geopolymer composites with fibers, as well as the results of testing the density, flexural strength and resistance to varying temperature cycles. In the case of fly ash-based composites, only rafia fiber has a positive effect on lowering the lambda coefficient, reducing the coefficient by 20%. The other fiber types negatively affect the thermal conductivity coefficient. In the case of composites based on calcined carbonaceous shale, both rafia and field grass fibers resulted in an improvement in insulating performance. In contrast, wood fibers had a negative effect. When analyzing the effect of fiber length on the thermal conductivity coefficient, it is difficult to determine the effect of fiber length and relationships. The length of rafia fibers had the greatest effect because, in the case of slate-based composites, long fibers were more favorable and in the case of ash-based matrix, short fibers were more favorable. The addition of fibers had no significant effect on the density changes of the composites. In the case of the coal shale-based matrix, the fibers caused a maximum density change of 3% by weight, while in the case of the Bełchatów ash-based matrix, the changes

Table 3. Results of density and thermal conductivity tests

	RD.B	RD.Ł	RK.B	RK.Ł	TD.B	TD.Ł	TK.B	TK.Ł	DD.B	DD.Ł	REF.B	REF.Ł
Conductivity coefficient [W/mK]	0.7292	0.6570	0.5516	0.8405	0.7314	0.7768	0.7365	0.8552	0.6949	0.9940	0.6881	0.9646
Density [kg/m <sup>3</sup> ]	1468.7	1641.7	1431.9	1618.4	1497.8	1655.4	1422.6	1566.1	1439.4	1595.7	1432.8	1606.4
Flexural strength [MPa]	1.69	5.75	1.81	4.65	2.22	5.57	1.83	4.95	2.01	5.02	1.98	5.70
Flexural strength after the climatic chamber [MPa]	1.39	4.23	1.70	4.76	1.93	5.94	1.21	4.94	1.33	4.13	1.66	4.02

amounted to a maximum of 4.5% by weight. Flexural strength tests showed that composites produced on the basis of calcined carbon slate showed higher strengths. All the fibers introduced into the composites due to the poor quality of the connection to the matrix did not have a positive effect on the flexural strength of the composites. The effect of varying temperature cycles reduced the flexural strength mainly for composites based on fly ash from the Bełchatów Power Plant.

fibers by chemical treatment. This type of treatment was not chosen due to the fact that geopolymerization is a process where alkalis are used and the curing process takes quite a long time. It was decided to see if the fibers without prior treatment would be “etched” just during the geopolymerization process. Based on SEM observations and on the results of flexural strength tests, it can be concluded that prior treatment is also necessary for the addition of fibers in geopolymerization processes.

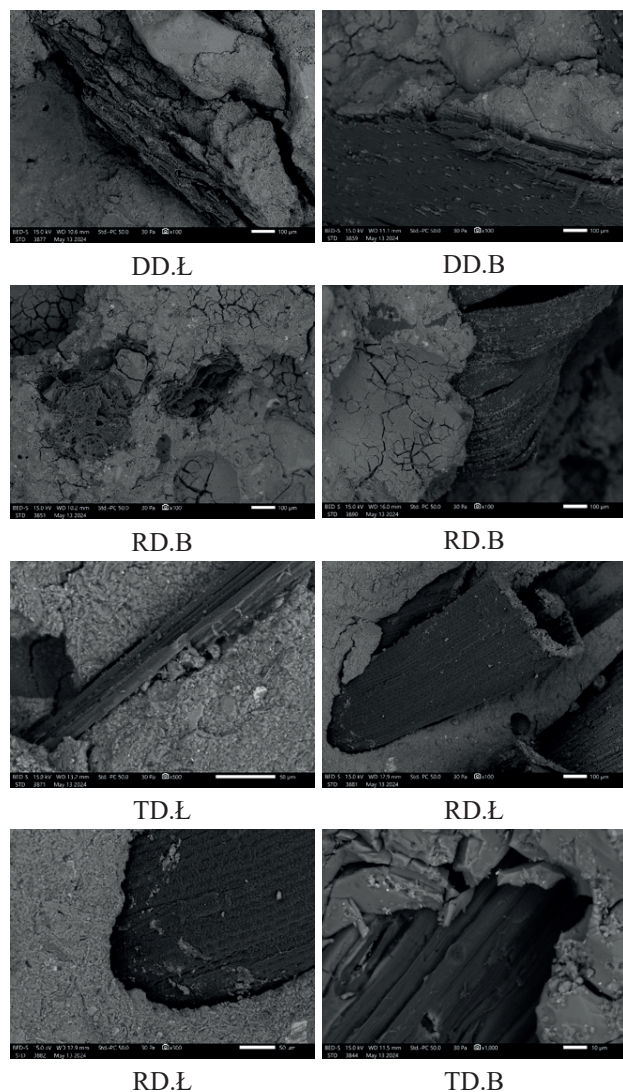


Fig. 3. Selected SEM microphotographs showing the quality of the fiber-axial bond

Based on the observation of the microstructure (Fig. 3) of the fabricated composites and, in particular, the observation of the contact zone between the fiber and matrix, it can be concluded that all composites were characterized by a very weak bonding at the fiber-matrix interface. In each case, voids between the fiber and matrix and lack of cohesion are visible. This is a result of the lack of prior preparation of the



Fig. 4. Appearance of samples after 500 cycles in UV chamber (accelerated aging tests) – RD.B. samples

Accelerated aging tests in a UV chamber showed no negative effect of UV radiation on the degradation rate of the composites. The evaluation was made by visually comparing the condition of the fibers and matrix surfaces. No surface loss or exfoliation was observed and fibers that were exposed and exposed to UV radiation did not degrade. Both natural fibers and matrix are resistant to the kind of factors used in this study (UV, rain, condensation). Examples of samples with visible reinforcement, after aging tests are shown in Figure 4.

#### 4. CONCLUSIONS

The article presents the results of a study of geopolymer composites based on two waste materials found in Poland in significant quantities. The composites were reinforced by introducing 1% fibers such as wood fibers, field grass fibers, raffia fibers. The fibers were introduced in the form of long fibers with a length of 5-7 cm and chopped short fibers with a length

of 1-1.5 cm. Studies were conducted on the effect of fiber addition on such properties of the composites as flexural strength, thermal conductivity coefficient, resistance to varying temperature cycles, density, resistance to UV radiation, rain and condensation. The results obtained allow the following conclusions:

1. Natural fibers introduced into geopolymer composites should be treated to etch and get rid of some organic matter. This conclusion is confirmed by an analysis of the literature [19-25]. The use of untreated fibers results in a very poor quality of the bond at the fiber-ossein interface. Even the strongly alkaline reaction of the activating solutions does not cause the fibers to bond well to the geopolymer matrix. This results in no effect of added fibers on the flexural strength of the composites. Untreated fibers even cause a reduction in strength properties due to a reduction in the active cross-sectional area of the matrix. The flexural strength values of RD.Ł, TD.Ł samples are comparable to those of the

reference sample, while the ash samples showed a slight decrease or comparable values after the introduction of fibers. However, the intended effect resulting in improved properties was not achieved.

2. Rafia fiber has the most favorable effect on insulating properties and thermal conductivity coefficient. Field grass fibers and wood fibers can adversely affect the insulating properties by increasing the heat conduction coefficient. This is probably related to the absorbency of these fibers [32].
3. All the fibers used are resistant to UV radiation, rain simulation and condensation. Accelerated aging tests showed no degradation of the fibers in the geopolymer matrix. The geopolymer matrix itself also shows significant resistance to UV radiation, rain simulation and condensation.
4. Coal shale-based geopolymers have significantly better strength parameters compared to fly ash-based geopolymers. They also show greater resistance to variable temperature cycles.

## REFERENCES

- [1] Davidovits J.: *30 Years of Successes and Failures in Geopolymer Applications*. Market Trends and Potential Breakthroughs. In Proceedings of the Geopolymer 2002 Conference, Melbourne, 2002, pp. 1-16.
- [2] Provis J.L., van Deventer J.S.J.: *Geopolymers: Structure, Processing, Properties, and Industrial Applications*. A volume in Woodhead Publishing Series in Civil and Structural Engineering, Woodhead Publishing: Cambridge, 2009.
- [3] Sharma U., Gupta N., Bahrami A., Özkılıç Y.O., Verma M., Berwal P., Althaqafi E., Khan M.A., Islam S.: *Behavior of Fibers in Geopolymer Concrete: A Comprehensive Review*, Buildings 14 (1) (2024), pp. 1-28. DOI: <https://doi.org/10.3390/buildings14010136>.
- [4] Bazan P., Kozub B., Łach M., Korniejenko K.: *Evaluation of Hybrid Melamine and Steel Fiber Reinforced Geopolymers Composites*, Materials 13 (23) (2020), pp. 1-15. DOI: <https://doi.org/10.3390/ma13235548>.
- [5] Łach M., Kluska B., Janus D., Kabat D., Pławicka K., Korniejenko K., Guigou M.D., Choińska M.: *Effect of Fiber Reinforcement on the Compression and Flexural Strength of Fiber-Reinforced Geopolymers*, Applied Sciences, 11 (21) (2021), 1–21. DOI: <https://doi.org/10.3390/app112110443>.
- [6] de Azevedo A.R.G., Cruz A.S.A., Marvila M.T., de Oliveira L.B., Monteiro S.N., Vieira C.M.F., Fediuk R., Timokhin R., Vatin N., Daironas M.: *Natural Fibers as an Alternative to Synthetic Fibers in Reinforcement of Geopolymer Matrices: A Comparative Review*, Polymers 13 (15) (2021), 1-21. DOI: <https://doi.org/10.3390/polym13152493>.
- [7] Viskovic A., Łach M., Hojdys Ł., Krajewski P., Kwiecień A.: *Experimental research on new sustainable geopolymer concretes reinforced and not reinforced with natural fibers*. Building for the Future: Durable, Sustainable, Resilient: proceedings of the fib Symposium 2023, Springer Nature, 2023, pp. 329-338. DOI:10.1007/978-3-031-32519-9\_31.
- [8] Viskovic A., Łach M., Hojdys Ł., Krajewski P., Kwiecień A.: *Experimental research on new sustainable geopolymer concretes reinforced and not reinforced with natural fibers*. Proceedings of the International Conference of Steel and Composite for Engineering Structures : ICSCES 2022, Springer, 2023, pp. 149-160. DOI:10.1007/978-3-031-24041-6\_12.
- [9] Korniejenko K., Łach M., Dogan-Saglamtimur N., Furtos G., Mikuła J.: *The overview of mechanical properties of short natural fiber reinforced geopolymer composites*, Environmental Research and Technology, 3 (1) (2020), pp. 28-39. DOI:10.35208/ert.671713.
- [10] Korniejenko K., Łach M., Hebdowska-Krupa M., Mikuła J.: *Impact of flax fiber reinforcement on mechanical properties of solid and foamed geopolymer concrete*, Advances in Technology Innovation, 6 (1) (2021), pp. 11-20. DOI:10.46604/aiti.2021.5294.
- [11] Gholampour A., Danish A., Ozbakkaloglu T., Yeon J.H., Gencil O.: *Mechanical and durability properties of natural fiber-reinforced geopolymers containing lead smelter slag and waste glass sand*, Construction and Building Materials, 352 (2022), 1-20. DOI: <https://doi.org/10.1016/j.conbuildmat.2022.129043>.
- [12] Bariş K.E., Tanaçan L.: *Durability behavior of banana fiber-reinforced natural pozzolan geopolymer*, Journal of Green Building, 18 (4) (2023), 49-168. DOI: <https://doi.org/10.3992/jgb.18.4.149>.

- [13] Asim M., Uddin G.M., Jamshaid H., Raza A., Tahir Z.R., Hussain U., Satti A.N., Hayat N., Arafat S.M.: *Comparative experimental investigation of natural fibers reinforced light weight concrete as thermally efficient building materials*, Journal of Building Engineering, 31 (2020), pp. 1-11. DOI: <https://doi.org/10.1016/j.jobbe.2020.101411>.
- [14] Daza-Badilla L., Gómez R., Díaz-Noriega R., Avudaiappan S., Skrzypkowski K., Saavedra-Flores E.I., Korzeniowski W.: *Thermal Conductivity in Concrete Samples with Natural and Synthetic Fibers*, Materials, 17 (4) (2024), pp. 1-21. DOI: <https://doi.org/10.3390/ma17040817>.
- [15] Łach M., Mierzwiński D., Korniejewo K., Miłkuła J.: *Geopolymer foam as a passive fire protection*. MATEC Web of Conferences, Fire and Environmental Safety Engineering, 2018, pp. 1-6. DOI: 10.1051/mateconf/201824700031.
- [16] Mohamed O., Zuaier H.: *Fresh Properties, Strength, and Durability of Fiber-Reinforced Geopolymer and Conventional Concrete: A Review*, Polymers 16 (1) (2024), 1-50. DOI: <https://doi.org/10.3390/polym16010141>.
- [17] Lv C., Liu J., Guo G., Zhang Y.: *The Mechanical Properties of Plant Fiber-Reinforced Geopolymers: A Review*, Polymers 14 (19) (2022), pp. 1-22. DOI: <https://doi.org/10.3390/polym14194134>.
- [18] Addis L.B., Sendekie Z.B., Satheesh N.: *Degradation Kinetics and Durability Enhancement Strategies of Cellulosic Fiber-Reinforced Geopolymers and Cement Composites*, Advances in Materials Science and Engineering, (2022), pp. 1-22. DOI: <https://doi.org/10.1155/2022/1981755>.
- [19] Omoniyi T.E., Akinyemi B.A.: *Durability based suitability of bagasse cement composite for roofing sheets*, Journal of Civil Engineering and Construction Technology, 3 (11) (2012), pp. 280-290. DOI: 10.5897/JCECT12.041.
- [20] Ramakrishna G., Sundararajan T., Kothandaraman S.: *Evaluation of durability of natural fibre reinforced cement mortar composite—a new approach*, ARPN Journal of Engineering and Applied Sciences, 5 (6) (2010), pp. 44-51.
- [21] Javadi A., Srithep Y., Pilla S., Lee J., Gong S., Turng L.S.: *Processing and characterization of solid and microcellular PHBV/coir fiber composites*, Materials Science and Engineering: C, 30 (5) (2010), pp. 749-757. DOI: <https://doi.org/10.1016/j.msec.2010.03.008>.
- [22] Bilba K., Arsene M.A.: *Silane treatment of bagasse fiber for reinforcement of cementitious composites*, Composites Part A: Applied Science and Manufacturing, 39 (9) (2008), pp. 1488-1495. DOI: <https://doi.org/10.1016/j.compositesa.2008.05.013>.
- [23] Claramunt J., Ardanuy M., García-Hortal J.A., Filho R.D.T.: *The hornification of vegetable fibers to improve the durability of cement mortar composites*, Cement and Concrete Composites, 33 (5) (2011), pp. 586-595. DOI: <https://doi.org/10.1016/j.cemconcomp.2011.03.003>.
- [24] Pehanich J.L., Blankenhorn P.R., Silsbee M.R.: *Wood fiber surface treatment level effects on selected mechanical properties of wood fiber–cement composites*, Cement and Concrete Research, 34 (1) (2004), pp. 59-65. DOI: [https://doi.org/10.1016/S0008-8846\(03\)00193-5](https://doi.org/10.1016/S0008-8846(03)00193-5).
- [25] de Lima T.E.S., de Azevedo A.R.G., Marvila M.T., Candido V.S., Fediuk R., Monteiro S.N.: *Potential of Using Amazon Natural Fibers to Reinforce Cementitious Composites: A Review*, Polymers 14 (3) (2022), pp. 1-20. DOI: <https://doi.org/10.3390/polym14030647>.
- [26] Lv C., Liu J.: *Alkaline Degradation of Plant Fiber Reinforcements in Geopolymer: A Review*, Molecules 28 (4) (2023), pp. 1-22. DOI: <https://doi.org/10.3390/molecules28041868>.
- [27] Abbas A-G.N., Aziz F.N.A.A., Abdan K., Nasir N.A.M., Huseien G.F.: *Experimental study on durability properties of kenaf fibre-reinforced geopolymer concrete*, Construction and Building Materials, 396 (2023), pp. 1-23. DOI: <https://doi.org/10.1016/j.conbuildmat.2023.132160>.
- [28] Qin L., Yan J., Zhou M. et al.: *Mechanical properties and durability of fiber reinforced geopolymer composites: A review on recent progress*, Engineering Reports, 5 (12) (2023), pp. 1-22. DOI: 10.1002/eng2.12708.
- [29] Liu J., Lv C.: *Durability of Cellulosic-Fiber-Reinforced Geopolymers: A Review*, Molecules, 27 (3) (2022), pp. 1-23. DOI: <https://doi.org/10.3390/molecules27030796>.
- [30] ASTM G-155 – Standard Practice for Operating Xenon Arc Lamp Apparatus for Exposure of Materials <https://www.astm.org/g0155-21.html> (Accessed 15 June 2024).
- [31] PN-EN 12390-5:2019-08 – Testing of concrete – Part 5: Flexural strength of test specimens <https://sklep.pkn.pl/pn-en-12390-5-2019-08p.html> (Accessed 15 June 2024).
- [32] Lilargem Rocha D., Tambara Júnior L.U.D., Marvila M.T., Pereira E.C., Souza D., de Azevedo A.R.G. A.: *Review of the Use of Natural Fibers in Cement Composites: Concepts, Applications and Brazilian History*, Polymers, 14 (10) (2022), pp. 1-22. DOI: <https://doi.org/10.3390/polym14102043>.

## Funding

This work was funded by the National Center for Research and Development in Poland under grant: M-ERA.NET3/2021/70/GEOSUMAT/2022 “Materials for Circular Economy – Industrial Waste Based Geopolymers Composites with Hybrid Reinforcement” under M-ERA.NET 3 Call 2021.





# ANALYSIS OF THE DEFORMATION OF ROAD SURFACE CONSTRUCTION BASED ON MONITORING CLIMATIC FACTORS

## ANALIZA ODKSZTAŁCEŃ KONSTRUKCJI NAWIERZCHNI DROGI NA PODSTAWIE MONITORINGU CZYNNIKÓW KLIMATYCZNYCH

Marek Iwański, Grzegorz Mazurek\*, Przemysław Buczyński  
Kielce University of Technology, Poland

### Abstract

The article presents the results of simulation of the deformation state of a road surface structure intended for traffic categories KR 3-4. Climatic factors such as temperature and humidity were obtained from a database collected based on the installed monitoring. The performed validation of the deformation state indicated a very good fitness of the model to the experimental results, provided that the viscoelastic model. The results indicated that the difference in pavement load time between 1 s and 1200 s in summer may result in an increase in horizontal deformation under the asphalt layer by 949%, and in winter by 74%. The calculated vertical displacement in winter after 1200 seconds of loading is equivalent to the displacement calculated after 1 second of loading the road surface in summer.

**Keywords:** pavement diagnostic, visco-elastic model, climatic factors monitoring

### Streszczenie

W artykule przedstawiono wyniki symulacji stanu odkształcenia konstrukcji nawierzchni drogowej przeznaczonej dla kategorii ruchu KR 3-4. Informacje na temat czynników klimatycznych takich jak temperatura oraz wilgotność pozyskano z prowadzonego monitoringu. Wykonana walidacja stanu odkształcenia wskazała na bardzo dobre dopasowanie modelu do wyników eksperymentu pod warunkiem zastosowania modelu lepkosprężystego. Wyniki symulacji wskazują, że różnica czasu obciążenia nawierzchni pomiędzy 1 s a 1200 s w okresie lata może spowodować wzrost odkształcenia poziomego pod warstwą asfaltową względnie o 94%, natomiast w okresie zimy o 74%. Obliczone przemieszczenie pionowe w okresie zimy po 1200 s trwania obciążenia jest równoważne z przemieszczeniem obliczonym po 1 s obciążenia nawierzchni drogowej w okresie lata.

**Słowa kluczowe:** diagnostyka nawierzchni, model lepkosprężysty, monitoring czynników klimatycznych

### 1. INTRODUCTION

In Poland, the bespoke design of the surface structure system is based on the assumption that a single load from a design axis of 100 kN causes exceedingly small deformations. For this reason, an adequate model for the analysis of the stress and deformation state of the flexible surface, is the elastic model defined for a load time of 0.02 s (vehicle speed of approximately

60 km/h) and an equivalent temperature of +13°C. Catalogue of typical flexible and semi-rigid pavements was developed for such reference conditions[1].

The issue related to measuring the deformation condition escalates in the case of using innovative materials. Their impact on the deformability in some cases differs from the information contained in the Catalogue. In spite of the fact, Polish legal system

\*Kielce University of Technology, Poland, e-mail: [gmazurek@tu.kielce.pl](mailto:gmazurek@tu.kielce.pl)

allows for the potential use of viscoelastic models, which permit the incorporation of load time in the design process [2]. There are numerous locations along the route of a road where the vehicles move at a low speed, and consequently, this results in load durations which are considerably longer than the design value provided for in the aforementioned Catalogue. In such case, the significant phenomenon of the relaxation of the rigidity modulus of the construction layers is of key importance for consideration, in particular at the design stage of a road repair or reconstruction project. An examination of the deformation state of the surface structure may be carried out on a case-by-case basis [1]. In order to achieve this purpose, it is absolutely crucial to possess knowledge of the mechanical characteristics of the materials that constitute the road surface structure [3, 4]. In result, the use of the viscoelastic model allows for a more precise design of structures where the load duration is relatively large during the summer period, such as, for instance: bus bays, road intersections. Afterwards, there is a possibility to run a series of simulations with various materials in order to achieve the optimal configuration. This article presents the results of a simulation of the deformation state taking into account the temperature and loading time using a viscoelastic physical design of the structural layers. Furthermore, the results were subject to validation of the condition of deformation of the terrain, based on the data obtained from the monitoring system installed on section of the road under surveillance.

**2. METHODS AND MATERIALS**

The analysis focuses on the deformation state of the road surface, the construction was carried out during the Techmatstrateg I project [5]. Under the project,

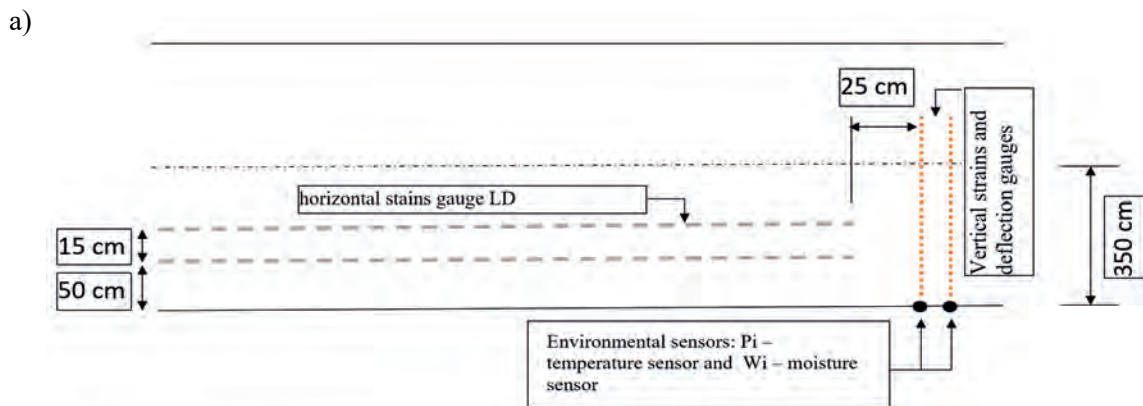
the construction with the following arrangement was constructed:

- wearing/binding layer made using SMA-JENA, grammage 8 cm;
- the substructure layer constructed using deep cold recycling technology (FRCM) with foamed asphalt and a dedicated mixed adhesive grammage 20 cm;
- ground substrate at bearing capacity group G1.

The substructure layer was a mixture of deep recycled (FRCM) with foamed asphalt [5]. It was manufactured with the use of an innovative mixed binder as part of the TECHMATSTRATEG I project. Detailed information on the application of this specific binder and the optimisation process is presented in the works [5, 6]. The layer subject to wear and serving as a binder was made using the innovative SMA-JENA mineral-asphalt mix instead of the traditional two-layer system. The SMA-JENA layer was prepared in line with the recommendations specified in the work [7].

**2.1. Monitoring system sensor diagram and the layout of structural layers**

Data on environmental factors were gathered by monitoring the experimental section situated within the premises of the organic fertiliser production and sand extraction facility Z.W.P. „MOSTY” sp. z o.o., where the main objective focused primarily on observing changes in the deformation state at significant points in the surface structure. An assembly of fibre optic sensors was embedded in two sections where the effects of the mixed binder was tested [6, 8]. The monitoring data was complemented by the recordings of environmental parameters, precisely meaning temperature and humidity. Monitoring set manufactured by SHM System®. A diagram of the layout of sensors (installation) is presented in Figure 1 [5].



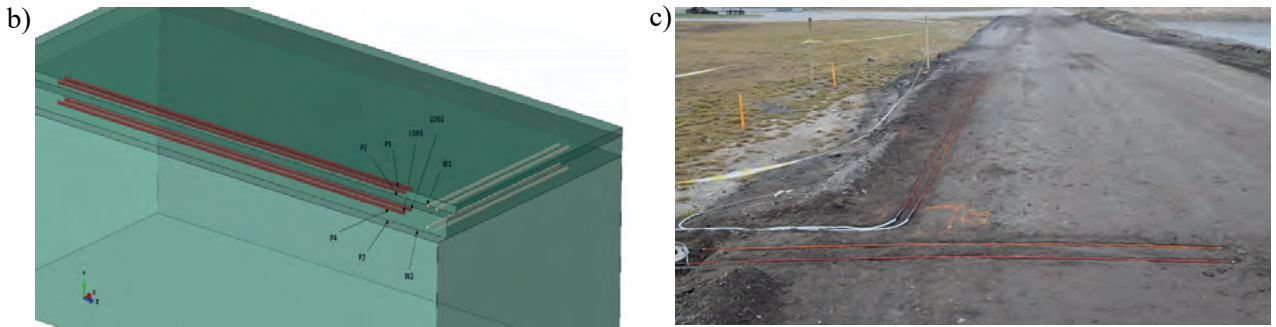


Fig. 1. Surface monitoring system: a) sensor installation diagram (top view); b) isometric view; c) optical fibre installation

**2.2. An analysis of alterations in climatic factors in relation to surface construction**

The scope of the monitored climatic factors included measurements of temperature and humidity. The temperature measurement covered the period ranging from the beginning of 2020 to February 2024. The temperature was recorded at 3 locations of the recycled substructure (bottom and middle of the FRCM, the SMA-JENA junction with the FRCM, and at a height of 1 m above the ground surface). Figure 2 presents a diagram of the temperature fluctuation situated at the contact point between the SMA-JENA layer and the FRCM (P2 sensors in accordance with Fig. 1b), depending on the month.

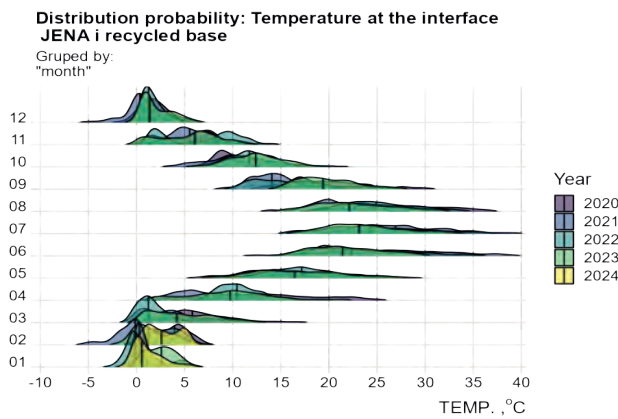


Fig. 2. The distribution of temperature at the contact area of the SMA-JENA surface and the recycled substructure (P2 sensors as shown in Fig. 1b)

Due consideration shall be given to the fact that during the 4 years of continuous surface monitoring, a slight displacement of the median result (horizontal line) towards higher temperatures (green and yellow) can be detected. Such result brings a dual implication. The initial implication is that the progressive warming of the climate is reflected by the value of the surface temperature. The second meaning, significantly more acute, the increase in temperature will cause a decrease

in the stiffness modulus of structure layers which will manifest itself as an increased accumulation of plastic deformation on the surface.

For the purpose of determining the distribution of deformation of the road surface structure, it was necessary to define the conventional temperature levels at the surface of the SMA-JENA layer and in the centre of the FRCM substructure layer. Their graphical visualisation is presented in Figure 3.

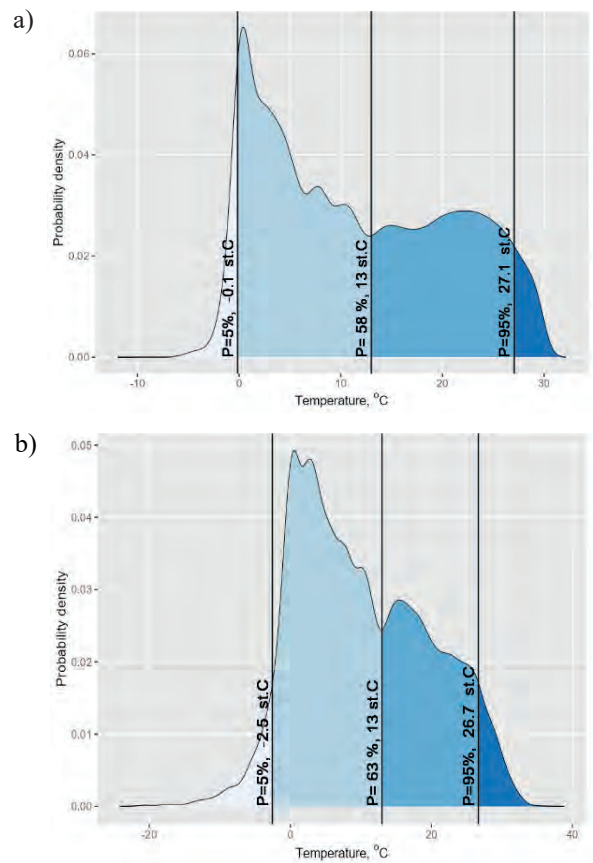


Fig. 3. Temperature distribution across the surface layer: a) FRCM; b) JENA

It was determined that for further analyses the “low” temperature will be represented by the temperature

corresponding to the 5% quantile of the probability distribution. However, the “high” temperature will be represented by the temperature taken from the 95% quantile of the probability distribution. In the case of the FRCM layer (Fig. 3a), the “low” temperature value was represented by  $-0.1^{\circ}\text{C}$ , whereas the “high temperature” was  $27.1^{\circ}\text{C}$ . In the case of the SMA-JENA layer (Fig. 3b), the temperature value labelled as “low” equalled  $-2.5^{\circ}\text{C}$ . Conversely, the “high” temperature equalled  $26.7^{\circ}\text{C}$ . In the case of the FRCM layer, the determination of the probability distribution function was based on the results of temperature measurements at the top surface of the JENA layer ( $h = 0\text{ cm}$ ), in the middle ( $h = 10\text{ cm}$ ) and at the bottom ( $h = 20\text{ cm}$ ). In addition, Figure 3 indicates the probability of the reference temperature occurring in Poland for asphalt surfaces of  $+13^{\circ}\text{C}$ . The divergence from the mean value may imply a potential requirement for its validation in view of the constant rise in temperature gradient observed, among others, within the segment subject to experiments.

**3. ANALYSIS OF THE SURFACE STRUCTURE DEFORMATION CONDITION**

The assessment of the deformation condition took into account a range of linear viscoelasticity, omitting the non-linear effects dependent on the stress level [9, 10]. A generalised Maxwell model (labelled as GM) for linear viscoelasticity (LVE) was taken into account as an adequate model for describing the material stress relaxation phenomenon [11]. The process of identifying the GM model parameters entailed

a concurrent effort to minimise the discrepancy between the experimental outcomes of the dynamic module and the phase shift angle, in comparison with the modelled results. A comprehensive compilation of the results of identifying parameters in the GM model, presented as a leading curve pertinent to the behaviour of the FRCM substructure and SMA-JENA layer is presented in Table 1.

The model parameters obtained in Table 1 were subject to validation and presented in works [5, 8, 12]. It must be clearly noted that the validation of the numerical model is not the focus of this paper (the results of the deformation measurements from the field tests are not presented here), however it was presented in the work [8]. The simulation of surface deformation was conducted for a load duration of 1s (brief period) and 1200 s (prolonged load period) utilising the parameters of the GM model as presented in Table 1. The statistical analysis results depicted in Figure 3 were utilised for temperature. The state of “low” temperature consisted in designating  $-2.5^{\circ}\text{C}$  to the SMA-JENA layer and  $-0.1^{\circ}\text{C}$  to the FRCM layer. Conversely, the state of “high” temperature consisted in assigning a temperature of  $+26.7^{\circ}\text{C}$  to the SMA-JENA layer, whereas the FRCM layer:  $+27.1^{\circ}\text{C}$ . It must be noted that the temperature of asphalt surfaces in Poland can achieve levels as high as  $+60^{\circ}\text{C}$  [13]. Such variant was not taken into analysis as the monitoring did not record a  $>40^{\circ}\text{C}$  temperature reading on the surface of SMA-JENA. Furthermore, there was approximately a 5% chance of temperatures exceeding  $+25^{\circ}\text{C}$ . In the case of the specified numerical model, the fundamental

Table 1. The leading curve parameters based on the relaxation function of the generalized Maxwell model for the SMA-JENA layer and FRCM at the reference temperature of  $13^{\circ}\text{C}$

Technology type	Generalised Maxwell model parameters		$\alpha$ , coefficient (WLF formula)	
	$G_i$ [-]	$\tau_i$ [s]	$C_1$	$C_2$
FRCM recycled substructure	$G_1 = 0.229$ $G_2 = 0.193$ $G_3 = 0.193$ $G_4 = 0.193$ $G_5 = 0.193$	$\tau_1 = 0.00097$ $\tau_2 = 0.08296$ $\tau_3 = 5.06899$ $\tau_4 = 213.756$ $\tau_5 = 12007.6$	7.1	67.1
	$G_0 = 11421\text{ MPa}$			
	$R^2 = 0.97; \text{RMSE} = 5.3\%$			
SMA-JENA wearing/binding layer	$G_1 = 0.252$ $G_2 = 0.252$ $G_3 = 0.222$ $G_4 = 0.177$ $G_5 = 0.096$	$\tau_1 = 0.00085$ $\tau_2 = 0.06414$ $\tau_3 = 2.79957$ $\tau_4 = 110.362$ $\tau_5 = 6066.03$	32.4	229.8
	$G_0 = 18060\text{ MPa}$			
	$R^2 = 0.99; \text{RMSE} = 7.8\%$			

dimensions of the FEM grid component were  $0.2 \times 0.2 \times 0.2$  m. In respect of the contact area (where the wheels of a vehicle remain in contact with the surface of the road), the dimensions of the component were reduced to  $0.04 \times 0.04 \times 0.04$  m. Furthermore, the segmentation was determined in such a way that for the following layers: SMA\_JENA and FB-RCM, their thickness dimension was divided into at least four parts (solid elements) in accordance with the conclusions drawn in work [4]. The eight-node linear shape function C3D8R was used as the shape function. The computational vehicle was weighted in such a manner as to produce a load of 850 kPa on the rear wheel for each axle. Conversely, the front axle wheel generated a surface pressure of 475 kPa. An exemplary horizontal simulation for “high” temperatures in the form of E22 deformation maps are presented in Figure 4.

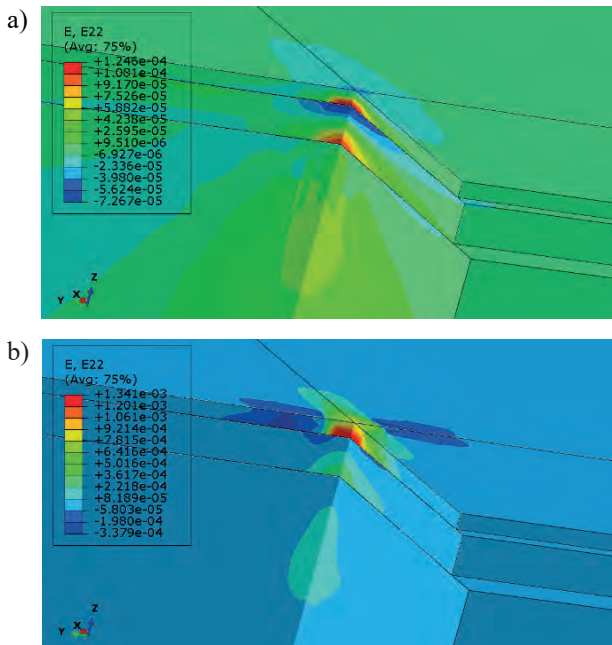


Fig. 4. E22 deformations (in parallel with the axis of the road – Y-Y axis) for “high” temperatures: a) applicable for a duration of a load of 1 s; b) applicable for a load duration of 1200 s

For the purpose of carrying out an accurate diagnosis of the surface, the duration of the load and the temperature of the surface must be taken into account. Due to that fact, the elastic model, while it is commonly implemented, is characterised by a limited use when addressing intricate surface loading scenarios in favour of the viscoelastic model. The viscoelastic Maxwell model is used to determine the detailed horizontal strain values at different depths of the road surface at the load application point, as summarised in Figure 5.

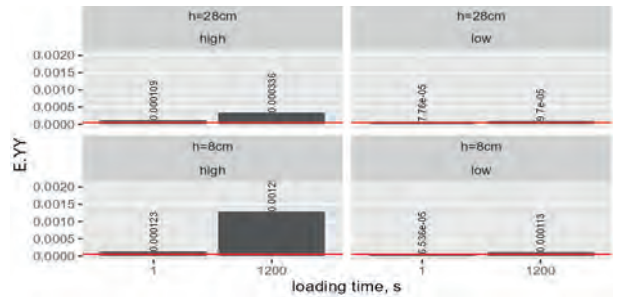


Fig. 5. Detailed readings of simulated  $E_{YY}$  deformation at the point of application of a vehicle wheel load of 850 kPa

Upon examination of the results presented in Figure 5, attention must be paid to the fact that the SMA-JENA layer displays significantly greater stiffness in comparison to the FRCM substructure layer in a low-temperature environment. In connection, the value of the deformation in the substructure has been reduced. At high temperatures, the stiffness modulus of SMA-JENA, which contains a large amount of asphalt, was significantly reduced. Its increased susceptibility causes significant deformations in the substructure, which may potentially initiate multiple cracks at its base. At the same time, the forming concentration of deformations at the bottom of the asphalt layer will likely initiate a sequence of net-like cracks on the asphalt’s surface in the spring and autumn seasons. In Figure 5, the red horizontal line represents the secure LVE range ( $100 \mu\epsilon$ ) for asphalt layers. Comparing its value to the displacement values during summer temperatures, it must be concluded that in case of recurring loads on the surface for a duration of 1200 s, there exists a significant probability of accumulation of plastic deformations.

Another characteristic associated with the deformability of the surface was the vertical shift at the location where the load was applied. It allows for a rapid evaluation of the degradation level of all surface layers. A statement of the Uzz vertical displacement results is presented in Figure 6.

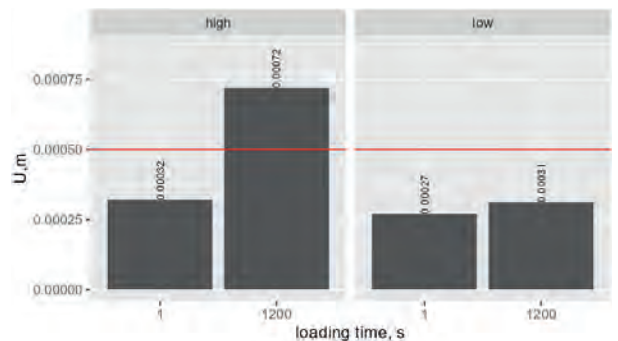


Fig. 6. Comprehensive readings of the simulated deformation of  $E_{YY}$  at the location where the vehicle wheel’s load of 850 kPa was applied

The analysis of the results presented in Figure 6 leads to the conclusion that the duration of the load application significantly influences the surface deflection during periods of high temperatures. Under low temperature conditions, the duration of 1200 s led to a relative increase of deformation by 15%, whereas during the summer, it increased by 125%. Without a doubt, this was caused, as previously mentioned, by a drastic decrease in the stiffness module of the SMA-JENA layer, of a greater significance than in the case of FRCM layer. Taking into account the requirements of the Polish Catalogue of Reconstructions and Renovations of Flexible and Semi-Rigid Surfaces [14] the maximum deflection value should be  $< 0.5$  mm for KR4 category roads. Hence, during the summer season, vehicles which put pressure on the surface for brief durations ( $< 1$  s) meet the criteria. Conversely, in the winter season, the duration of safe application of pressure can be significantly prolonged. Pursuant to the simulation, the surface deflection during winter season after 1200 s is comparable to the surface stress applied in the summer season for the duration of 1 s.

In summary, the duration for which the load is applied significantly impacts the deformability of the surface and it is influenced by the surface temperature. Considering the aforementioned two factors, the deformation state of the surface can be precisely mirrored, and its deformability can be tailored to real-world conditions based on lab material tests. Unfortunately, the traditional elastic model for materials containing asphalt binder is inadequate for such tasks and it displays the behaviour of the surface layers for a precisely outlined operational scheme of a road surface construction.

## REFERENCES

- [1] „Załącznik do Zarządzenia nr 31 GDDKiA z 16.06.2014, Katalog Typowych Konstrukcji Nawierzchni Podatnych i Półsztywnych.” Politechnika Gdańska, 2014.
- [2] Dz.U. 1999 nr 43 poz. 430, *Rozporządzenie Ministra Transportu i Gospodarki Morskiej z dnia 2 marca 1999 r. w sprawie warunków technicznych, jakim powinny odpowiadać drogi publiczne i ich usytuowanie (in Polish)*, nr Dz.U. 1999 nr 43 poz. 430.
- [3] Judycki J. i in., *Analizy i projektowanie konstrukcji nawierzchni podatnych i półsztywnych*, Warszawa, Wydawnictwa Komunikacji i Łączności, 2014.
- [4] Nagórski R.T., Błażejowski K., *Mechanika nawierzchni drogowych w zarysie*, Warszawa, Wydawnictwo Naukowe PWN, 2014.
- [5] TECHMATSTRATEG I, *The innovative technology used the binding agent optimization that provides the long service life of the recycled base course*, National Centre for Research and Development (NCBR), TECHMATSTRATEG1/349326/9/NCBR/2017, 2018.
- [6] Mazurek G., Iwanski M., *Optimisation of the innovative hydraulic binder composition for its versatile use in recycled road base layer*, IOP Conference Series: Materials Science and Engineering, t. 603, s. 032044, wrz. 2019, doi: 10.1088/1757-899X/603/3/032044.
- [7] Błażejowski K., Strugała I., *Nawierzchnie jednowarstwowe z SMA 16 JENA*, Rettenmaier Polska, 2nd Edition, 2019.

## 4. CONCLUSIONS

Based on the conducted studies and examinations, the subsequent detailed conclusions were drawn:

- Utilising data from the strain and displacement state monitoring affirmed the high effectiveness of the implemented modelling with the generalized Maxwell model to elucidate the relaxation phenomenon in recycled mixtures.
- Temperature monitoring has shown an increase in the mean temperature in the period from 2020 to 2024, which is due to climate warming. Thus, the conventional equivalent temperature used for surface design of  $+13^{\circ}\text{C}$  might possibly require a review in specific regions of Poland in the future. With the probability of 95% that the temperature in the analysed layers of road surface construction did not exceed  $+27.1^{\circ}\text{C}$  in the summer season and was lower than  $-2.5^{\circ}\text{C}$  in the winter season. The peak summer temperature observed at the SMA-JENA layer's surface was lower than  $+40^{\circ}\text{C}$ .
- During the summer season, the horizontal deformation at the bottom layer of SMA-JENA increased by 73% between the pressure application duration of 1s and 1200 s, whereas in the summer it increased by 94%. This fact must be taken into account when designing surface structures subject to heavy vehicle traffic in junctions characterised by low freedom of movement.
- For the examined road structure solution meant for KR3-4 traffic, the deflection in winter for the application of a load for a duration of 1200 s was comparable to the deflection of the same surface in the summer season for the duration of 1 s.

- [8] Mazurek G., Buczyński P., Mackiewicz P., Iwański M., *Field investigation of a deep recycled base course layer containing dedicated three component hydraulic and bituminous binder*, Construction and Building Materials, t. 390, s. 131685, sie. 2023, doi: 10.1016/j.conbuildmat.2023.131685.
- [9] Read J., Whiteoak D., Hunter R.N., *The Shell Bitumen handbook*, 5th ed. London: Thomas Telford, 2003.
- [10] Mazurek G., Pszczoła M., Szydłowski C., *Non-linear mastic characteristics based on the modified mscr (multiple stress creep recovery) test*, Structure and Environment, t. 11, nr 1, Art. nr 1, mar. 2019, doi: 10.30540/sae-2019-002.
- [11] Mazurek G., *Analysis of selected properties of asphalt concrete with synthetic wax*, Bulletin Of The Polish Academy of Sciences Technical Sciences, t. 66, nr 2, Art. nr 2, 2018, doi: 10.24425/122102.
- [12] Mazurek G., Buczyński P., Iwański M., Podsiadło M., *Thermal Analysis-Based Field Validation of the Deformation of a Recycled Base Course Made with Innovative Road Binder*, Materials, t. 14, nr 20, Art. nr 20, paź. 2021, doi: 10.3390/ma14205925.
- [13] Piłat J., Radziszewski P., *Nawierzchnie asfaltowe: podręcznik akademicki*. Warszawa: Wydawnictwa Komunikacji i Łączności, 2010.
- [14] „Katalog przebudów i remontów nawierzchni podatnych i półsztywnych”. GDDKiA, IBDiM, 2013.



# THE IMPACT OF INTERNAL HYDROPHOBIZATION ON THE PROPERTIES OF THE CEMENT-BASED MATERIALS WITH MINERAL ADDITIVES

## WPŁYW HYDROFOBIZACJI OBJĘTOŚCIOWEJ NA WŁAŚCIWOŚCI MATERIAŁÓW CEMENTOWYCH Z DODATKAMI MINERALNYMI

Kalina Materak\*, Alicja Wieczorek, Marcin Zasada, Marcin Koniorczyk  
Lodz University of Technology, Poland

### Abstract

*The paper presents results regarding the possibility and effectiveness of carrying out the internal hydrophobization in cement-based materials with mineral additives such as granulated blast furnace slag, silica dust and silica fly ash. The obtained results indicate that effective internal hydrophobization by using triethoxyoctylsilane is achievable and provides protection against water by decreasing the capillary absorption of water in the material. However, it also affects the hydration process of the binder, which results in a reduction in the compressive strength of the material.*

**Keywords:** internal hydrophobization, triethoxyoctylsilane, granulated blast furnace slag, silica fly ash, silica fume

### Streszczenie

*W pracy przedstawiono wyniki dotyczące możliwości przeprowadzenia i skuteczności procesu hydrofobizacji objętościowej w materiałach cementowych z dodatkami mineralnymi, takimi jak: granulowany żużel wielkopiecowy, pył krzemionkowy oraz lotny popiół krzemionkowy. Otrzymane wyniki wskazują, że efektywna hydrofobizacja w masie wykonana przy pomocy trietoksyoktylosilanu jest osiągalna i zapewnia ochronę przed działaniem wody w postaci ograniczenia absorpcji kapilarnej w materiale. Jednakże wiąże się ona również z wpływem na proces hydratacji spoiwa, co skutkuje obniżeniem wytrzymałości na ściskanie materiału.*

**Słowa kluczowe:** hydrofobizacja objętościowa, trietoksyoktylosilan, granulowany żużel wielkopiecowy, mikrokrzemionka, popiół lotny

### 1. INTRODUCTION

The use of mineral additives in cement-based building materials, such as granulated blast furnace slag (ŻW), silica fly ash (PK) and silica fume (MK), can ensure many benefits and become more and more popular. Mentioned additives can improve the rheological properties of mixtures, prevent segregation of components and improve workability. Their use can provide develop in strength, impermeability and

corrosion resistance of the hardened material. The use of mineral additives allows for partial replacement of Portland cement CEM I, the production of which is associated with the emission of large amounts of carbon dioxide. As a result, the carbon footprint of the cement-based materials (composites) might be reduced and the negative impact on the environment is limited [1, 2]. Increasing the durability of cementitious building materials can also reduce their negative

\*Lodz University of Technology, Poland, e-mail: [kalina.grabowska@p.lodz.pl](mailto:kalina.grabowska@p.lodz.pl)



impact on the environment. Water and moisture are one of the factors causing degradation and destruction of porous building materials. One of the methods of protection them from water and improving their durability is hydrophobization. This is a process by which material acquires hydrophobic properties, i.e. is difficult to wet by water. Hydrophobic surfaces are characterized by a wetting angle above  $90^\circ$ . In case of building materials, the process of hydrophobization might be implemented on the surface or in the whole volume of the material, which is called internal hydrophobization. Surface hydrophobization consists in applying a hydrophobic agent only to the surface of the material. Hydrophobic properties are obtained only by the surface layer, due to the limited depth of penetration of the hydrophobic agents [3]. Internal hydrophobization ensures hydrophobicity of the material in its entire volume. It is performed by adding appropriate agents (usually in the form of admixtures) during the production of the material together with the batch water or in the end of mixing. Organosilicon compounds such as silicone resins, siloxanes or silanes can be used for hydrophobization [3]. In particular the latter might provide a highly effective protection against water in cementitious materials, as shown, for example, in [4-7]. There are only few papers in the scientific literature considering the internal hydrophobization of cementitious materials with mineral additives, performed by organosilicon compounds. The presented paper concerns the issue of possibilities and difficulties in performing internal hydrophobization by using triethoxyoctylsilane in cementitious materials with the addition of ground, granulated blast furnace slag, silica fume and silica fly ash. The paper presents results concerning the influence of the organosilicon hydrophobic admixture on the hydration of selected binders. The impact on the strength of the tested material after 2, 28, 56 and 90 days of curing was also determined. The effectiveness of the internal hydrophobization was examined by the capillary water absorption test.

## 2. MATERIALS AND METHODS

The ordinary Portland cement CEM I 42.5R with the following additives were used: granulated, ground blast furnace slag (ŻW), silica fume (MK) and silica fly ash (PK). Cement pastes and mortars with a water-binder ratio equal to 0.5 were prepared. River sand of fraction 0/2 mm was used. In pastes and mortars with the addition of granulated blast furnace slag, 50% of

the ordinary Portland cement was replaced by the above-mentioned mineral additive in accordance with the recommendations of the PN-EN 15167-1 standard [8]. In the case of silica fume (microsilica) 10% of the ordinary Portland cement was replaced according to the PN-EN 13263-1 standard [9]. In the material with silica fly ash the share of the additive was 25% in accordance with the recommendations of the PN-EN 450-1 standard [10]. Cement with the appropriate mineral additive was combined before putting into the batch water and mixed manually until the binders combined. Mortars were prepared in accordance with the PN-EN 196-1 standard [11]. In order to determine and analyze the possibility and effectiveness of internal hydrophobization by means of organosilicon compounds, a silicon-based hydrophobic admixture (DH) was used, the main component of which was triethoxyoctylsilane (Fig. 1). The properties and principles of use of the admixture are presented in Table 1. The dosage of 0.8% of the binder mass is recommended by the product manufacturer. The admixture was dosed to the mixing water. The applied water-binder ratio (0.5) allowed for the preparation of materials without the addition of a plasticizer.

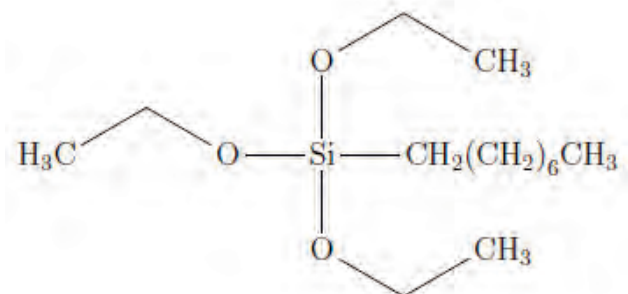


Fig. 1. Schematic chemical structure of triethoxyoctylsilane

Table 1. Principles of use and properties of a hydrophobic admixture

Main component	Dosage (%bm)	Solvent	Type of dispersion	Dosing method
Triethoxyoctylsilane	0.8%	Water	Emulsion	Batch water

Reference (REF\_ŻW, REF\_MK, REF\_PK) and internal hydrophobic samples (DH\_ŻW, DH\_MK, DH\_PK) were prepared. In order to determine the effect of the hydrophobic admixture on the binders hydration, a calorimetric tests were carried out in the TAM Air isothermal calorimeter at  $20^\circ\text{C}$  for 7 days according to the ASTM C 1679-08 standard

[12]. The test of capillary water absorption in the mortars was carried out in accordance with the PN-EN 1015-18 standard [13]. The compressive strength of hardened mortars after 2, 28, 56 and 90 days of curing was carried out according to the PN-EN 1015-11 standard [14]. Mortars samples with dimensions of 40 mm × 40 mm × 160 mm were demolded after 24 hours and stored in water for the first 14 days after demolding, and then in air-dry conditions ( $T = 20^{\circ}\text{C} \pm 2^{\circ}\text{C}$ ,  $\text{RH} = 55\% \pm 5\%$ ) until the test was performed. The implemented method of sample conditioning was aimed for activating the hydrophobic admixture [15]. Compressive strength after 2 days of mortars curing was determined on moist samples.

### 3. RESULTS AND DISCUSSION

#### 3.1. Isothermal calorimetry

The influence of the used hydrophobic organosilicon admixture on the hydration of the cement with mineral additives was determined by isothermal calorimetry. The rate of heat release is presented in Figure 2. Two samples of each pastes were tested. In general organosilicon compounds affect the hydration of binders by slowing down their hydration [16-19]. Triethoxyoctylsilane attaches to the surface of binder grains, thus hindering the access of water to the binder. Moreover, the organic, hydrophobic part of the compound, i.e. the octyl group, also repels water molecules. Organosilicon compounds might create a steric hindrance around the binder grains [2, 20], which is why they affect the amount and rate of heat released during the hydration process. The addition of a hydrophobic admixture to the mixing water caused changes in the heat release rate regardless of the used mineral additive, as shown in Figure 2. The silane-based admixture also caused a decrease in the amount of heat released after 7 days of testing. In the pastes with the addition of granulated blast furnace slag, the amount of heat released in the reference sample REF\_ŻW was 180.6 J/g. In the internal hydrophobic sample, it was reduced by 4.1% (to 173.3 J/g for DH\_ŻW). In the pastes with the addition of microsilica, the amount of heat released in the reference sample REF\_MK was 229.0 J/g. In the internal hydrophobic sample, it was reduced by 5.2% (to 225.4 J/g for DH\_MK). In the pastes with the addition of silica fly ash, the amount of heat released in the reference sample REF\_PK was 270.4 J/g. In the internal hydrophobic sample it was reduced by 1.6% (to 256.3 J/g for DH\_PK).

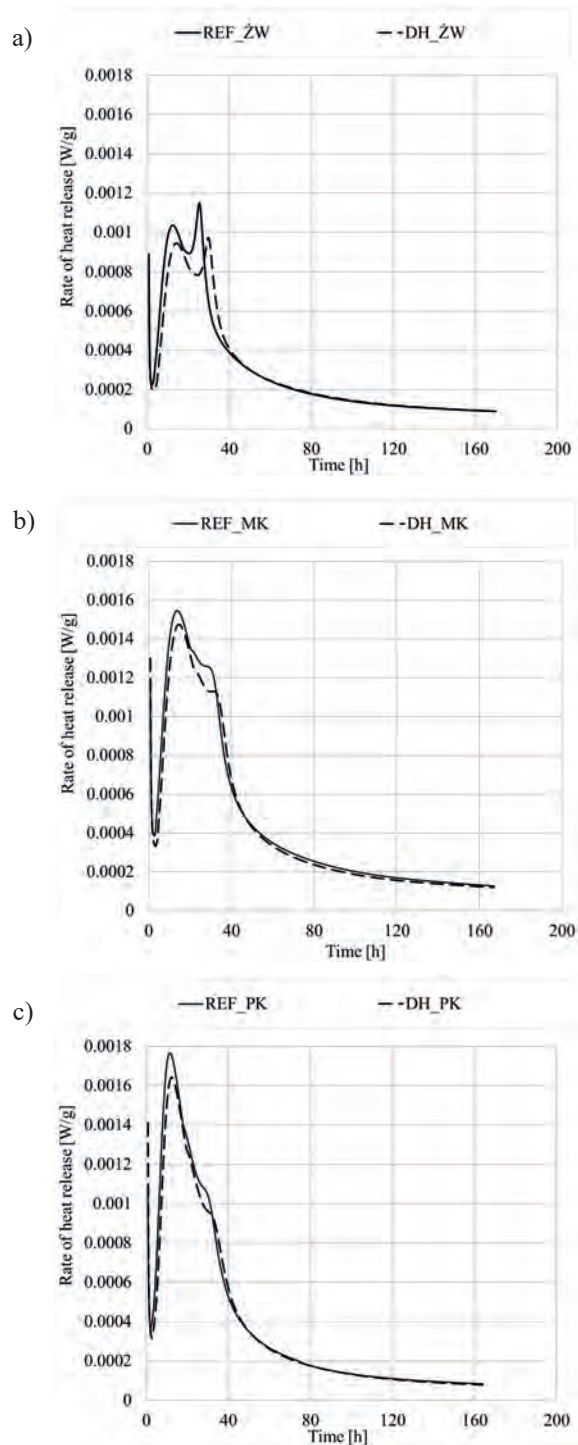


Fig. 2. The rate of heat release in pastes with a) granulated blast furnace slag, b) silica fume, and c) silica fly ash

#### 3.2. Capillary water absorption

The capillary water absorption test for mortars was carried out on 6 samples with dimensions of 40 mm × 40 mm × 80 mm. The side walls of the samples were covered by a silicone sealant to prevent water evaporation. The mortars were placed in water to

a depth of about 5 mm. The changes in the mass of the samples was measured after 10, 20, 30, 40, 50, 60, 90 minutes and 2, 3, 4, 5, 6 and 24 hours. The mass changes of the mortars are shown in Figure 3. The use of the silane-based hydrophobic admixture in the amount of 0.8% bm. ensured an effective reduction in water absorption in the mortars and a decrease in the capillary absorption coefficients. In case of mortar with the addition of granulated blast furnace slag, the capillary absorption coefficient of the reference sample (REF\_ŽW) was  $0.1063 \text{ kg/m}^2 \times \text{min}^{0.5}$ , and for the internal hydrophobic sample (DH\_ŽW) was reduced to  $0.0195 \text{ kg/m}^2 \times \text{min}^{0.5}$ , (by 81.6%). For mortar with the addition of microsilia, the capillary absorption coefficient was reduced by 67.0% (from  $0.0633 \text{ kg/m}^2 \times \text{min}^{0.5}$ , for REF\_MK to  $0.0208 \text{ kg/m}^2 \times \text{min}^{0.5}$ , for DH\_MK). In the reference mortar with the addition of silica fly ash (REF\_PK) the capillary absorption coefficient was  $0.0872 \text{ kg/m}^2 \times \text{min}^{0.5}$ , and it was reduced to  $0.0278 \text{ kg/m}^2 \times \text{min}^{0.5}$  (by 68.0%) for the hydrophobic sample DH\_PK.

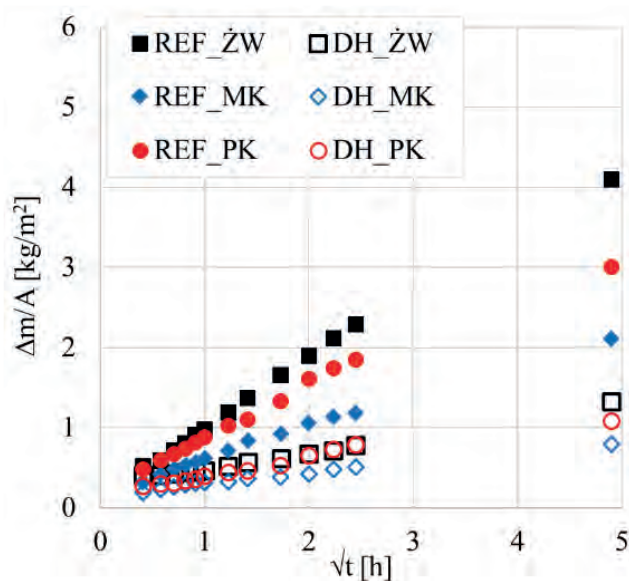


Fig. 3. Mass changes in mortars during capillary water absorption test

### 3.3. Compressive strength

Table 2 presents the results of compressive strength of mortars after 2, 28, 56 and 90 days of curing. Six samples of each type of mortar were tested. The use of the organosilicon hydrophobic admixture resulted in a decrease in compressive strength. For internal hydrophobic mortar with the addition of granulated blast furnace slag (DH\_ŽW), the strength was reduced by 7.0% after 2 days, by 4.3% after 28 days, by 9.6%

after 56 days and by 9.2% after 90 days of curing in relation to the reference samples (REF\_ŽW). In the case of hydrophobic mortar with the addition of silica fume (DH\_MK), the compressive strength was reduced by 25.7% after 2 days, by 27.1% after 28 days, by 26.6% after 56 days and by 25.0% after 90 days of curing in relation to the reference samples (REF\_MK). In internal hydrophobic mortar with silica fly ash added (DH\_PK), a decrease in strength by 5.2% after 2 days, by 23.9% after 28 days, by 8.5% after 56 days and by 10.7% after 90 days of curing was observed in relation to the reference samples (REF\_PK).

Table 2. Compressive strength of mortars after 2, 28, 56 and 90 days of curing

Sample/Test time	Compressive strength [MPa]			
	2 days	28 days	56 days	90 days
REF_ŽW	5.5	39.7	42.6	45.6
DH_ŽW	5.1	38.0	38.5	41.4
REF_MK	16.1	63.2	64.8	72.5
DH_MK	12.0	46.0	47.6	54.4
REF_PK	10.5	45.0	45.5	45.8
DH_PK	10.0	34.2	41.6	40.9

## 4. CONCLUSIONS

The presented paper investigated and analyzed the effectiveness of the internal hydrophobization and its impact on the basic properties of porous cementitious materials with mineral additives such as: granulated blast furnace slag, microsilia and silica fly ash. The obtained results indicate that internal hydrophobization of cementitious materials with mentioned mineral additives by means of triethoxyoctylsilane is possible and provides effective protection against water penetration into the material. However, dosing of the organosilicon hydrophobic admixture together with the mixing water affects the binder hydration process, which is visible as a reduction in the amount and rate of heat release. As a consequence, a decrease in the strength of the internal hydrophobic mortars is also observed even after 90 days of curing. The obtained results indicate that internal hydrophobization of cementitious materials with mineral additives is possible and effective, although this topic requires further research.

## REFERENCES

- [1] Kurdowski W.: *Chemistry of cement and concrete*. Wydawnictwo Naukowe PWN, Warszawa 2010.
- [2] Neville A.M.: *Properties of Concrete*. Stowarzyszenie Producentów Cementu, Kraków 2012.
- [3] Barnat-Hunek D.: *Surface free energy as a factor affecting effectiveness of hydrophobisation in protection of building construction*. Politechnika Lubelska, Lublin 2016.
- [4] Materak K., Wieczorek A., Łukowski P., Koniorczyk M.: *The influence of internal hydrophobization using organosilicon admixture on the performance and the durability of concrete*. Cement Wapno Beton, XXVIII, 4, 2023, 225-237, DOI: <https://doi.org/10.32047/CWB.2023.28.4.2>.
- [5] Zhang Ch., Zhang S., Yu J., Kong X.: *Water absorption behavior of hydrophobized concrete using silane emulsion as admixture*. Cement and Concrete Research, 154, 2022, 106738, DOI: <https://doi.org/10.1016/j.cemconres.2022.106738>.
- [6] Moriconi G., Tittarelli F., Corinaldesi V.: *Review of silicone-based hydrophobic treatment and admixtures for concrete*. Indian Concrete Journal, LXXVI, 10, 2002, 637-642.
- [7] Zhu Y., Kou S., Poon C., Dai J., Li Q.: *Influence of silane-based water repellent on the durability properties of recycled aggregate concrete*. Cement and Concrete Composites, 35, 2013, 32-38, DOI: <https://doi.org/10.1016/j.cemconcomp.2012.08.008>.
- [8] Norma PN-EN 15167-1 Mielony granulowany żużel wielkopieczowy do stosowania w betonie, zaprawie i zaczynie – Część 1: Definicje, specyfikacje i kryteria zgodności, 2007.
- [9] Norma PN-EN 13263-1 Pył krzemionkowy do betonu – Część 1: Definicje, wymagania i kryteria zgodności, 2006.
- [10] Norma PN-EN 450-1 Popiół lotny do betonu – Część 1: Definicje, specyfikacje i kryteria zgodności, 2012.
- [11] Norma PN-EN 196-1 Metody badania cementu – Część 1: Oznaczanie wytrzymałości, 2016.
- [12] ASTM C 1679-08 Standard Practice for Measuring Hydration Kinetics of Hydraulic Cementitious Mixtures Using Isothermal Calorimetry, 2009.
- [13] Norma PN-EN 1015-18 Metody badań zapraw do murów – Część 18: Określenie współczynnika absorpcji wody spowodowanej podciąganiem kapilarnym stwardniałej zaprawy, 2003.
- [14] Norma PN-EN 1015-11 Metody badań zapraw do murów – Część 11: Określenie wytrzymałości na zginanie i ściskanie stwardniałej zaprawy, 2020.
- [15] Aldred J.M., Swaddiwudhipong, S., Lee S.L., Wee T.H.: *The effect of initial moisture content on water transport in concrete containing a hydrophobic admixture*. Magazine of Concrete Research, 53, 2001, 127-134, DOI: <https://doi.org/10.1680/mac.2001.53.2.127>.
- [16] Feng H., Thanh Nam Le H., Wang S., Zhang M.: *Effects of silanes and silane derivatives on cement hydration and mechanical properties of mortars*. Construction and Building Materials, 2016, 129, 48-60, DOI: <https://doi.org/10.1016/j.conbuildmat.2016.11.004>.
- [17] Grabowska K., Koniorczyk M.: *Influence of organosilicon admixtures on the hydration of Portland cement*. Journal of Thermal Analysis and Calorimetry, 2022, 147, 6131–6145, DOI: <https://doi.org/10.1007/s10973-021-10978-x>.
- [18] Stoch A., Zdaniewicz M., Paluszkiwicz Cz.: *The effect of polymethylsiloxanes on hydration of clinker phases*. Journal of Molecular Structure, 511–512, 1999, 319-325.
- [19] Kong X.M., Liu H., Lu Z.B., Wang D.M.: *The influence of silanes on hydration and strength development of cementitious systems*. Cement and Concrete Research, 67, 2015, 168-178, DOI: <https://doi.org/10.1016/j.cemconres.2014.10.008>.
- [20] Łukowski P.: *Domieszki do zapraw i betonów*. Polski Cement Sp. z o.o., Kraków 2003.

## Acknowledgements

*Funding: This research did not receive any specific grant from funding agencies in the public, commercial, or not-for-profit sectors.*



# ASSESSMENT OF AGGREGATE MIXTURE REACTIVITY IN CONCRETE AT 60°C

## OCENA REAKTYWNOŚCI MIESZANINY KRUSZYW W BETONIE W TEMPERATURZE 60°C

Kinga Dziedzic\*, Michał A. Glinicki  
Institute of Fundamental Technological Research,  
Polish Academy of Sciences, Warsaw, Poland

### Abstract

Research on the durability of structural concrete requires careful selection of aggregates, particularly considering their reactivity to alkali-silica reaction (ASR). The Miniature Concrete Prism Test (MCPT) allows for shortened testing time and eliminates the need for aggregate crushing, making it a practical alternative to other methods. The aim of the research is to evaluate the reactivity of aggregate mixtures with varying mineral compositions. Research results confirm the significant impact of fine aggregates on concrete expansion in the MCPT method in NaOH solution at 60°C. The observed expansion correlates with a reduction in concrete's elastic modulus.

**Keywords:** alkali-silica reaction (ASR), concrete expansion, MCPT method, fine aggregate, durability

### Streszczenie

Badania nad trwałością betonu konstrukcyjnego wymagają starannej selekcji kruszyw, szczególnie uwzględniającej ich reaktywność na reakcję alkalia-krzemionka (ASR). Metoda Miniature Concrete Prism Test (MCPT) pozwala na skrócenie czasu badania i eliminację konieczności rozdrabniania kruszywa, co czyni ją praktyczną alternatywą dla innych metod. Celem badań jest ocena reaktywności mieszaniny kruszyw o zróżnicowanym składzie mineralnym. Wyniki badań potwierdzają znaczący wpływ kruszywa drobnego na ekspansję betonu w metodzie MCPT w roztworze NaOH w temp. 60°C. Obserwowana ekspansja koreluje z redukcją modułu sprężystości betonu.

**Słowa kluczowe:** reakcja alkalia-krzemionka (ASR), ekspansja betonu, metoda MCPT, kruszywo drobne, trwałość

### 1. INTRODUCTION

Designing concrete mixtures for durability in the operational conditions of engineering structures requires the selection of components considering the stability of their properties in aggressive environments. Mineral aggregates in cement concrete are generally components with unchanged mechanical properties. Exceptions include aggregates containing reactive silica minerals susceptible to reacting with sodium and

potassium hydroxides in the pore solution of cement concrete, known as the alkali-silica reaction (ASR). Their use in structural concrete can cause premature damage in the form of cracking, delamination, and swelling of elements, thereby reducing the operational suitability of the structure [1-2].

The selection of non-reactive aggregates is mainly conducted through petrographic analysis of the aggregate and analysis of potential concrete

\*Institute of Fundamental Technological Research, Polish Academy of Sciences, Warsaw, Poland, e-mail: [kdzie@ippt.pan.pl](mailto:kdzie@ippt.pan.pl)

expansion under conditions that accelerate the harmful effects of ASR. The classification of aggregate reactivity is generally performed separately for each aggregate fraction, especially distinguishing between coarse and fine aggregates. According to standard recommendations, identified reactivity in one of the aggregate fractions requires treating the entire aggregate mix the same way and applying appropriate measures to prevent ASR-induced damage. Alternatively, the reactive aggregate fraction should be replaced with a non-reactive one. This approach does not align with current trends in the sustainable use of mineral resources.

The role of fine aggregate reactivity sometimes raises controversy. Literature reports indicate that expansion due to ASR increases with decreasing aggregate grain size due to the increased surface area of reactive aggregate components. However, it has been found that this relationship is not monotonic for some mineral aggregates, and the greatest expansion occurs for intermediate fractions [3-4]. Due to the dependence of reactivity on grain size, aggregates should be classified based on tests of the same fractions that will be used in concrete without crushing them.

Worldwide and in Poland, the susceptibility of aggregates to the alkali-silica reaction is primarily classified using the accelerated 14-day method at 80°C (PB/1/18 [5]) and the 1-year method at 38°C (PB/2/18 [6]). However, both methods have their drawbacks. The accelerated method requires crushing the aggregate to 2 mm, making it difficult to accurately assess the reactivity of mixed aggregate fractions. The 1-year method is problematic due to intensive alkali leaching and the impractically long testing time. The problem

of alkali leaching from concrete specimens in sealed containers occurs due to water condensation on the specimens' surfaces, leading to outward alkali diffusion from the concrete's interior and causing reduced prism expansion [7]. The Miniature Concrete Prism Test (MCPT) [8], standardized in 2019, aims to eliminate the drawbacks of the above methods with a relatively short testing time (8 weeks) without the need to crush coarse aggregate. In laboratory studies [9, 10], the MCPT method showed good agreement with the 1-year method and, more importantly, better agreement with the measurements of ASR effects on concrete blocks exposed to natural climatic conditions [11].

The aim of the research is to assess the reactivity of aggregate mixtures for concrete, composed of fine and coarse aggregate fractions with diverse mineral compositions. The research scope includes coarse crushed aggregate from solid rock and naturally occurring fine aggregates (sands). Alongside the PB/1/18 [5] methodology, the MCPT methodology was applied, i.e., the procedure for testing the expansion of concrete samples exposed to a 1 M NaOH solution at 60°C.

## 2. MATERIALS AND RESEARCH METHODS

For the tests, coarse crushed aggregate from greywacke (S) and amphibolite (A) with fractions of 2/8 and 8/16 were used. Natural quartz sands (B, W, T) and a mixture of natural sands (X) with a grain size of up to 2 mm were used as fine aggregates. The selection of sand was justified by the variation in potential alkali reactivity (Table 1). Portland cement CEM I 52.5 R with an alkali content of  $\text{Na}_2\text{O}_{\text{eq}} = 0.88$  was used to make the concrete. Table 2 presents the chemical composition of the cement.

Table 1. Mineral aggregate characteristics

Symbol	Aggregate type	Density [g/cm <sup>3</sup> ]	Expansion acc. to PB/1/18 [5] [%]	
			14-day	28-day
S	Greywacke gravel	2.71	0.31	0.52
A	Amphibolite gravel	2.89	0.16	0.26
B	Natural pit sand	2.65	0.09	0.23
W	Natural riverbed sand	2.66	0.30	0.46
T	Natural pit sand	2.65	0.36	0.57
X	Sand mixture (50% mass of B+50% mass of W)	2.66	0.16	0.32

Table 2. Cement composition in accordance with PN-EN 196-2

Cement type	Constituent [%]								
	SiO <sub>2</sub>	Al <sub>2</sub> O <sub>3</sub>	Fe <sub>2</sub> O <sub>3</sub>	CaO	MgO	SO <sub>3</sub>	Na <sub>2</sub> O	K <sub>2</sub> O	LOI
CEM I 52.5 R	19.42	5.45	2.94	64.10	1.75	3.50	0.24	0.97	1.03

Concrete mixtures were designed according to the MCPT procedure [8], with a limitation on the coarse aggregate grain size to 12.5 mm. The aggregate mix was composed of appropriate fractions of gravel and sand. The fine aggregate was used without altering the grain size, and the missing 2/4 mm fraction was filled with 2/4 mm coarse aggregate. The amount of cement was constant, 420 kg/m<sup>3</sup>, the water-cement ratio (w/c) equaled 0.45; sodium hydroxide was added to the mixing water to increase the alkali content to Na<sub>2</sub>O<sub>eq</sub> = 1.25%. A modification of the procedure was the use of a mixture of aggregates with different reactivities.

Samples with gauge studs were formed from each mixture, each measuring 50 × 50 × 285 mm. The samples were compacted on a vibrating table and stored in molds at high humidity (RH > 95%) for 24 hours. The samples were then placed in water at 60°C for 24 hours, after which they were immersed in a 1 molar sodium hydroxide solution and stored for 84 days. Reference samples were stored in water at 20-22°C during the same period.

Periodically, measurements of the expansion of the samples and the resonant modulus of elasticity of the concrete were carried out using a GrindoSonic MK5 device with a piezoelectric detector, similar to [12]. At the end of the tests, compressive strength was measured on 50 mm cubic samples cut from the concrete beams.

### 3. RESULTS AND DISCUSSION

Table 3 presents a summary of the expansion test results and the compressive strength measurements of concrete after the expansion tests, as well as the reference samples stored in water at 20°C. The values are averages from three samples, with a variation not exceeding ±11%.

Figure 1 shows the change in length of the concrete samples over time during exposure to a 1 molar sodium hydroxide solution at 60°C. According to the MCPT procedure, the criteria for aggregate reactivity are as follows: expansion of concrete samples after 8 weeks of exposure up to 0.03% corresponds to non-reactive aggregate, 0.03-0.12% to moderately reactive, and 0.12-0.24% to highly reactive. Based on MCPT criteria, the coarse aggregates tested, even when compared with non-reactive sand B, fall into the category of moderately reactive aggregates. It was observed that replacing non-reactive quartz sand (B) with another natural sand of higher potential reactivity (Table 1) resulted in a significant increase in concrete expansion, reaching up to 110%.

Greywacke aggregate is recognized in the literature as potentially reactive [13], except for deposits in New Zealand. The primary reason for their reactivity is the presence of reactive minerals such as microcrystalline and cryptocrystalline quartz [14]. Especially when exposed to de-icing agents, greywacke aggregates significantly contribute to concrete degradation, manifesting as considerable cracking and a substantial reduction in the modulus of elasticity [15].

Amphibolite aggregates found in Poland are considered non-reactive, as confirmed by observations of currently used concrete structures. However, literature data [13] indicate that among the main minerals in amphibolite, there may be hornblende, plagioclase, quartz, epidote, calcite, and titanite, with quartz, chlorite, and calcite present in the veins. The reactive phase of amphibolite is primarily microcrystalline quartz, and also cryptocrystalline quartz found in veins and shear zones. Both the type and amount of reactive minerals ultimately influence the aggregate's susceptibility to reaction with sodium and potassium hydroxides in concrete.

Table 3. Summary of concrete samples expansion and compressive strength measurements

Mix	Expansion in 1 M NaOH at 60°C [%]		Compressive strength [MPa] after exposure to	
	56-day	84-day	NaOH 60°C	H <sub>2</sub> O 20°C
SB	0.065	0.092	57.2	59.0
SW	0.093	0.119	64.3	73.1
ST	0.120	0.158	64.2	73.9
AB	0.048	0.075	56.6	67.6
AX	0.069	0.115	55.5	63.8
AW	0.095	0.159	51.9	66.5

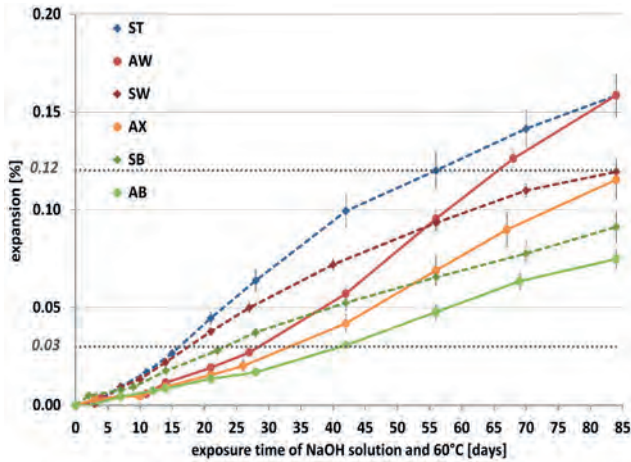


Fig. 1. Expansion of concrete specimens during exposure to NaOH solution and 60°C

For all aggregate mixtures, the effect of the fine aggregate used on the final expansion of concrete samples was observed – greater potential reactivity of the sand leads to greater final expansion of the aggregate mixture in the MCPT. Replacing non-reactive quartz sand (B) with potentially reactive sand (W) resulted in a moderate increase in expansion, about 20 – 30%, of concrete samples with greywacke (S), while with amphibolite (A) it was as much as 110%. A similar correlation, i.e., a significant influence of sand reactivity on the final expansion of concrete samples, was found in studies involving external alkali exposure [15]. In [16], river sand was identified as a cause of ASR damage in analyzed structures, and laboratory studies showed that depending on the type of non-reactive coarse aggregate used (limestone and granite), the classification of sand reactivity could change.

All concrete samples analyzed showed a decrease in the resonant modulus of elasticity and compressive strength of the concrete due to storage of the samples in a NaOH solution at 60°C (Fig. 2). The reduction in modulus of elasticity was greater with higher reactivity of the sand used in the aggregate mix. Samples with reactive sand (W), after being stored under ASR-promoting conditions, exhibited a significantly lower modulus of elasticity compared to samples with non-reactive sand – unlike the reference samples stored in water. In terms of compressive strength, no similar dependence was noted, although storage of samples under ASR-promoting conditions caused a significant decrease in strength – ranging from 2% to 15%.

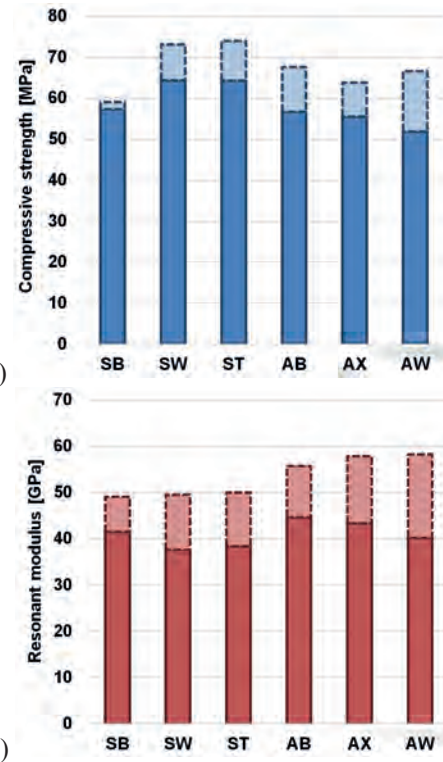


Fig. 2. Compressive strength (a) and resonant modulus of elasticity (b) of concrete after storing samples for 84 days under ASR-promoting conditions (solid line) and reference samples stored in water (dashed line)

The degree of deterioration in mechanical properties is a significant factor in assessing the risk associated with the occurrence of reactions [12]. Generally, all mechanical properties of concrete are expected to worsen due to the destructive effects of the alkali-aggregate reaction, and the degree of deterioration depends on the reactivity of the aggregate, the grain size, and the expansive properties of ASR products. Exposure of concrete samples to 60°C and high humidity in [17] showed a clear decrease in the modulus of elasticity by 21–36% and a moderate decrease in compressive strength by 7–14%. The current study results confirm this range of changes in mechanical properties and validate the varied susceptibility of these properties to ASR-induced damage – the modulus of elasticity of concrete is most closely correlated with the extent of damage due to the alkali-aggregate reaction in concrete.

#### 4. CONCLUSIONS

Based on the conducted research, the main conclusions are as follows:

1. The use of the “Miniature Concrete Prism Test” (MCPT) to assess the reactivity of a mixture of



different fractions of mineral aggregates with varying reactivities allows for the identification of the impact of fine fractions on concrete expansion due to ASR. The variability in the potential reactivity of natural quartz sands leads to a significant increase in concrete sample expansion, reaching up to 110% after 84 days of exposure to a NaOH solution at 60°C.

2. Concrete sample expansion in an ASR-promoting environment is correlated with a reduction in the

resonant modulus of elasticity. With increased potential reactivity of the natural sand used in the aggregate mix, there is a greater reduction in the modulus of elasticity of the concrete.

3. The method for determining aggregate reactivity in concrete using a 1 molar NaOH solution at 60°C allows for the categorization of reactivity in a manner similar to methods previously used in the country.

## REFERENCES

- [1] Owsiak Z., *Korozja wewnętrzna betonu*. Monografie, Studia, Rozprawy (M66). Wydawnictwo Politechniki Świętokrzyskiej, Kielce 2015.
- [2] Góralczyk S., Filipczyk M., *Aktualne badania reaktywności alkalicznej polskich kruszyw – część II*, [w:] Glapa W. (ed.) *Kruszywa Mineralne*, t. 2, Wydział Geoinżynierii, Górnictwa i Geologii Politechniki Wrocławskiej, Wrocław 2018, pp. 37-48.
- [3] Dunant C.F., Scrivener K.L., *Effects of aggregate size on alkali-silica reaction induced expansion*, *Cement and Concrete Research* 42 (6) (2012) pp. 745–751.
- [4] Multon S., Leklou N., Petit L., *Coupled effects of aggregate size and alkali content on ASR expansion*, *Cement and Concrete Research* 38 (3) (2008) pp. 350–359.
- [5] Procedura Badawcza GDDKiA PB/1/18 Instrukcja badania reaktywności kruszyw metodą przyspieszoną w 1 M roztworze NaOH w temperaturze 80°C. GDDKiA (2019).
- [6] Procedura Badawcza GDDKiA PB/2/18 Instrukcja badania reaktywności kruszyw w temperaturze 38°C według ASTM C1293/RILEM AAR-3. GDDKiA (2019).
- [7] Lindgård J., Andiç-Çakir O., Fernandes I., Rønning T.F., Thomas M.D.A., *Alkali-silica reactions (ASR): Literature review on parameters influencing laboratory performance testing*, *Cement and Concrete Research* 42 (2) (2021) pp. 223-243.
- [8] AASHTO T 380 Standard Method of Test for Potential Alkali Reactivity of Aggregates and Effectiveness of ASR Mitigation Measures (Miniature Concrete Prism Test, MCPT), American Association of State Highway and Transportation Officials, 2019.
- [9] Latifee E.R., Rangaraju P.R., *Miniature Concrete Prism Test: Rapid Test Method for Evaluating Alkali-Silica Reactivity of Aggregates*, *Journal of Materials in Civil Engineering*, Vol. 27, Issue 7, 2015.
- [10] Konduru H., Rangaraju P.R., *Amer O., Reliability of Miniature Concrete Prism Test in Assessing Alkali-Silica Reactivity of Moderately Reactive Aggregates*, *Transportation Research Record: Journal of the Transportation Research Board*, Vol. 2674, Issue 4, 2020.
- [11] Tanesi J., Drimalas T., Chopperla K.S.T., Beyene M., Ideker J.H., Kim H., Montanari L., Ardani A., *Divergence between Performance in the Field and Laboratory Test Results for Alkali-Silica Reaction*, *Transportation Research Record: Journal of the Transportation Research Board*, Vol 2674, Issue 5, 2020.
- [12] Dziedzic K., Glinicki M.A., *Risk assessment of reactive local sand use in aggregate mixtures for structural concrete*, *Construction and Building Materials*, 408, 2023, 133826.
- [13] Fernandes I., Ribeiro A.M., Broekmans M., Sims I., *Petrographic Atlas: Characterisation of Aggregates Regarding Potential Reactivity to Alkalis*, RILEM TC 219-ACS Recommended Guidance AAR-1.2, for use with the RILEM AAR-1.1 Petrographic Examination Method, Springer 2016.
- [14] Glinicki M.A., Józwiak-Niedźwiedzka D., Antolik A., Dziedzic K., Gibas K., *Podatność wybranych kruszyw ze skał osadowych na reakcję alkalia-kruszywo*, *Roads and Bridges - Drogi i Mosty*, 18, 1, 2019, pp. 5-24.
- [15] Glinicki M.A., Bogusz K., Józwiak-Niedźwiedzka D., Dąbrowski M., *ASR performance of concrete at external alkali supply – effects of aggregate mixtures and blended cement*, *International Journal of Pavement Engineering*, 24:1, 2023.
- [16] Deschenes R.A., Hale W.M., *Alkali-silica reaction in concrete with previously inert aggregates*, *Journal of Performance of Constructed Facilities*, 31 (2) (2019).
- [17] Hafci A., Turanlı L., Bektas F., *Wpływ rozszerzalności powodowanej reakcją kruszywa z wodorotlenkami sodu i potasu na właściwości mechaniczne betonu*, *Cement Wapno Beton*, 26(1) (2021), pp. 12-23.

## Funding

*This paper was funded by the National Science Centre as part of the Preludium project titled “Prediction of thermo-elastic properties of composite materials in the system of reactive silica with alkali metal hydroxides in the field of temperature and gamma irradiation” (2023/49/N/ST8/02157).*



# THE INFLUENCE OF CHLORIDE IONS CONTENT ON THE MECHANICAL PROPERTIES OF CONCRETE

## WPŁYW ZAWARTOŚCI JONÓW CHLORKOWYCH NA WŁAŚCIWOŚCI MECHANICZNE BETONU

Zofia Szweda\*  
Silesian University of Technology, Poland

### Abstract

*This paper presents an analysis of the effect of concrete salinity on the splitting tensile strength of specimens taken directly from the HC-500 floor slab and the flexural and compressive strength and the value of the modulus of elasticity of specimens made under laboratory conditions from lightweight concrete and ordinary concrete. The tests were carried out in two variants: in the first, chloride ions were introduced into the concrete by the migration method and in the second, as an additive introduced directly with the batch water. The analysis showed that the additive can affect certain mechanical properties of concrete both favorably and unfavorably. The results indicate that it is important to examine the issue of the influence of salinity on concrete's mechanical properties. This knowledge can be applied to the modeling of damage in reinforced concrete structures resulting from exposure to chloride-rich environments.*

**Keywords:** prestressed structures, HC-500 floor slabs, concrete salinity, concrete strength, chloride ions, modulus of elasticity

### Streszczenie

*W niniejszej pracy przedstawiono analizę badań wpływu zasolenia betonu na wytrzymałość na rozciąganie przy rozluźnianiu próbek pobranych bezpośrednio z płyty stropowej HC-500 oraz wpływu zasolenia na wytrzymałość na zginanie i ściskanie oraz na wartość modułu sprężystości próbek wykonanych w warunkach laboratoryjnych z betonu lekkiego i betonu zwykłego. Badania przeprowadzono w dwóch wariantach: w pierwszym po wprowadzeniu jonów chlorkowych do betonu metodą migracyjną w próbkach pobranych z płyt HC-500 i wykonanych z betonu lekkiego i w drugim, jako dodatek wprowadzony bezpośrednio z wodą zarobową w próbkach z betonu zwykłego. Przeprowadzone badania porównawcze różnych betonów z dodatkiem NaCl wykazały, że dodatek ten może wpływać zarówno korzystnie, jak i niekorzystnie na niektóre właściwości mechaniczne betonu. Przeprowadzone badania wskazują, że istotne jest dokładniejsze rozpoznanie zagadnienia wpływu zasolenia betonu na jego właściwości mechaniczne, co może być następnie wykorzystane w procesie modelowania zniszczeń konstrukcji żelbetowych wywołanych oddziaływaniem środowiska zawierającego chlorki.*

**Słowa kluczowe:** konstrukcje sprężone, płyty stropowe HC-500, zasolenie betonu, wytrzymałość betonu, jony chlorkowe, moduł sprężystości

### 1. INTRODUCTION

The impact of chloride ions on reinforced and prestressed concrete structures is complex in nature. It can pose a threat by destroying the cement matrix that forms the cover of the reinforcement, and also,

it can initiate corrosion and destruction of the steel reinforcement [1]. The mechanism of the effects of reinforcement corrosion on concrete cover is now fairly well understood, while the effects of chloride ions on the cement matrix in concrete and the impact of

\*Silesian University of Technology, Poland, e-mail: [zofia.szweda@polsl.pl](mailto:zofia.szweda@polsl.pl)

these effects on the mechanical properties of concrete are usually ignored. Even small amounts of chlorides, contained in soft drinking water (up to 0.3 mg/L), can cause corrosion of the reinforcement of water tanks under unfavorable conditions [2]. Other times, they can cause the formation of products that increase in volume due to crystallization, causing tensile stresses [3]. The whole range of processes that occur in concrete under the influence of chloride ions will undoubtedly affect its mechanical properties. However, not enough research defining these relationships exists.

The mechanical properties of concrete depend on two basic hydration products: hydrated calcium silicate (C-S-H) and calcium hydroxide (CH). Moreover, there is a relationship between the Ca/Si ratio of C-S-H and the mechanical properties of concrete [4]. In [5], the mechanical properties of various Self-Compacting Concrete (SCC) concrete mixtures prepared from two types of cement: OPC (ordinary Portland cement) and PPC (Portland pozzolanic cement) were evaluated. Compressive strengths were determined after 28, 90 and 360 days of curing, which were compared with the Ca/Si ratio calculated by energy dispersive X-ray spectroscopy (EDX) and the amount of calcium hydroxide (%) calculated by thermogravimetric analysis (TGA). The effect of NaCl salt added directly to the batch water during the making of the concrete mix at 0%, 1%, 3% and 5% (by weight of the batch water) was studied. A control SCC concrete mix (0% NaCl) was compared with SCC mixes with chloride admixture (1%, 3% and 5% NaCl) for a given cement type. It was observed that the compressive strength decreased for concrete from OPC mixes while it increased for PPC concrete with chloride ion content. The average decrease in compressive strength of concrete from OPC mixes was 10.88%, while the average increase in compressive strength of chloride-doped PPC concrete was 8.92% with respect to the control SCC concrete mix. Both the Ca/Si ratio and compressive strength increased with maturation time for OPC at different concentrations of NaCl. However, in PPC-based SCC concretes, the compressive strength increased, while the Ca/Si ratio decreased with concrete maturation time. In SCC concretes prepared with OPC, both the calcium hydroxide content and the Ca/Si ratio increased with maturation age, while the opposite relationship of these parameters was observed in SCC concretes prepared with PPC.

In [6], there are presented tests of compressive strength and Young's modulus carried out after 3, 7

and 28 days of maturation of samples with different chloride contents of 0.00, 0.07, 0.60 and 1.20% (of the weight of cement). However, no significant changes in the mechanical properties of concretes in the early maturation period dependent on the addition of NaCl were observed.

However, in [7], the destructive force determined in the study of mechanical fracture parameters carried out with the use of a so-called „Brazilian” method, using a central notch in the centre of the cylindrical test specimen, was about 15% lower after 30 days of natural diffusion in specimens made of high-strength HPPC concrete saturated with chloride ions than in control specimens from this concrete. In contrast, indirect tensile tests conducted using the Brazilian method showed no differences in the strength values obtained in concrete subjected to diffusion penetration of chloride ions and in reference concrete.

The impact of concrete salinity on its mechanical properties is particularly significant, especially when modeling the durability of reinforced concrete structures. Variations in concrete characteristics, influenced by chloride ions – such as strength and modulus of elasticity – can alter the nature and location of cracks within the concrete matrix. This aspect has been largely overlooked in current concrete cracking models, and there is a scarcity of experimental studies addressing this concern.

The main objective of this pilot research work was to test the possibility of the effect of chloride ions on the mechanical characteristics of concrete. The effect of salinity of concrete on the splitting tensile strength of specimens taken directly from the HC-500 slab and exposed to chloride ions in an electric field was tested. The effect of salinity caused by chloride ions in an electric field on the flexural and compressive strengths and the value of the modulus of elasticity of specimens made under laboratory conditions from lightweight concrete was also investigated. The effect of the addition of NaCl to the batch water on the splitting tensile strength and on the value of the modulus of elasticity of specimens made from lightweight concrete was evaluated.

## 2. MATERIALS AND METHODS

Three types of samples were prepared for testing: 1) 5 cylindrical specimens with a diameter of  $\varnothing 95$  mm and a height of 50 mm – taken with a crown drill directly from the HC-500 prestressed concrete slab; 2) 11 rectangular specimens with dimensions of  $40 \times 40 \times 160$  mm – made under laboratory conditions

from ready dry concrete mixture; 3) 6 cylindrical specimens with a diameter of Ø 150 mm and a height of 300 mm made from ordinary concrete with the addition of NaCl directly to the batch water (in the amount of 1.5% to the weight of cement) and 6 of the same specimens without the addition of NaCl. Since the study is preliminary and the results of analogous studies available in the literature do not give clear answers as to the effect of NaCl content on the mechanical properties of concrete, different types of concrete were chosen.

To determine the composition of the ready-mix lightweight concrete, a sieve analysis of the aggregate was performed and the cement content was determined roughly. A super-plasticizer was added according to the manufacturer’s recommendations. The preparation of beams for testing was carried out in accordance with PN-EN 196-1 [8]. The samples were unmoulded about 24 hours after the mixture was placed in the moulds. The finished beams were then left submerged in water for 56 days. Cylindrical specimens were cut from fragments of the floor, the age of which was determined to be 6 months at the time of testing based on the manufacturer’s data. Cylindrical samples prepared from ordinary concrete were stored under laboratory conditions at a temperature of about 20°C and were unmoulded after 28 days. The quantitative composition of the tested concretes is shown in Table 1.

Table 1. Composition of tested concretes

Constituent of concrete	Concrete in HC-500 slabs	Lightweight concrete	Ordinary concrete
	kg/m <sup>3</sup>		
Type of cement	CEM II A-S 52.5 R	CEM I 42.5 R	CEM I 42.5 R
Mass of Cement	581	577	350
Aggregate	1597	250	1788
Silica fume	65	–	–
Foam glass	–	1012.80	–
Superplasticizer	22.95	30	–
NaCl	–	–	5.29
Water	180	370	192.5
w/c	0.31	0.64	0.55
γ <sub>v</sub> kg/m <sup>3</sup> / Volume weight	2621	826.95	2460

Figure 1 shows the particle size distribution of the tested concretes.

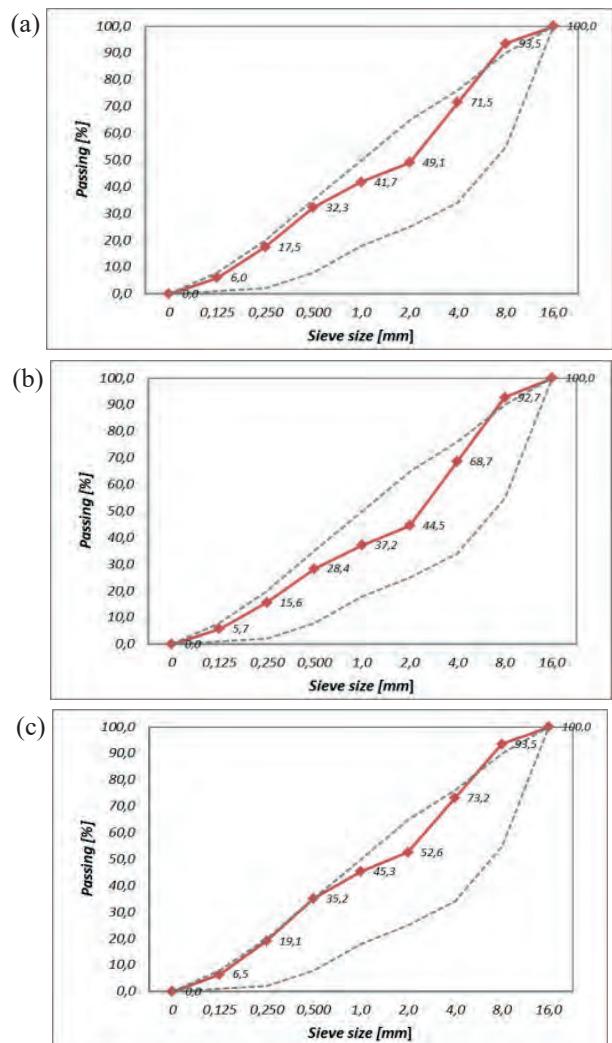


Fig. 1. Particle size distribution in: (a) HC-500 slab concrete and (b) lightweight concrete (c) ordinary concrete

Table 2 shows the chemical composition of the cements used.

Table 2. Chemical composition of the cements used

Components, % of mass	CEM I 42.5 R	CEM II A-S 52.5 R
SiO <sub>2</sub>	19.38	21.1
Al <sub>2</sub> O <sub>3</sub>	4.57	5.63
Fe <sub>2</sub> O <sub>3</sub>	3.59	3.59
CaO	63.78	59.3
MgO	1.38	2.24
K <sub>2</sub> O	0.58	0.59
Na <sub>2</sub> O	0.21	0.6
Eq. Na <sub>2</sub> O	0.59	0.2
SO <sub>3</sub>	3.26	2.86
Cl	0.069	0.039

Figure 2 shows slabs with sampling locations for testing (2a) and a view of the slabs after sampling (2b). The sampling location was determined by taking into account the possibility of cutting the samples without reinforcement and the technical conditions for setting up the drilling rig. After cutting, the bottom surface of the samples was levelled with a diamond saw, setting the height of the samples at 50 mm.

In order to analyze the effect of salinity on the properties of concrete, an accelerated migration process of chloride ions assisted by an electric field was carried out. Prior to the migration process, both cylindrical samples cut from HC-500 slabs and cuboidal samples were stored in water for 72 hours. Two-plastic reservoirs with an epoxy resin-protected side surface (2) were tightly attached to the top surface of the cylindrical specimens (which is also the top edge of the ceiling) (1), and filled with a 3% NaCl solution. Perpendicular specimens (3) were similarly

prepared, the side walls secured with waterproof glue and the previously prepared plastic tanks (4) slid onto the elements.

Cathodes (5) made of stainless steel and sized to fit the cross-section of the test piece were placed in the tanks filled with water, on a grid anode (6) made of platinum-coated titanium. The system was connected to a direct current source of  $U = 18\text{ V}$  (8). The electrical circuit was powered by a special bridge (7), which ensured stabilization of the flowing current and also distributed the voltage between the electrodes. The cylindrical samples were connected to the circuit for a period of one month, during which the NaCl solution was changed three times. Throughout the test period, the temperature of the solutions was constant at around  $20^{\circ}\text{C}$  – Figure 3a.

Perpendicular samples were tested for a week, during which the NaCl solution was replaced once after 3 days – Figure 3b.

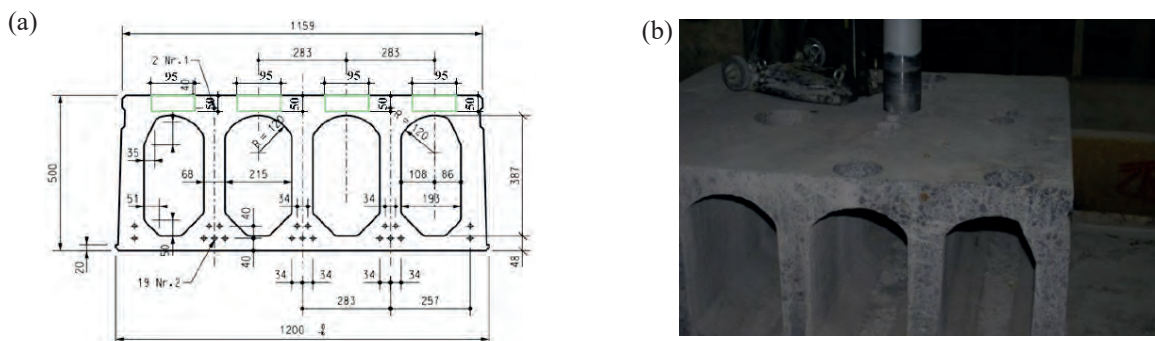


Fig. 2. (a) Drawing of the disc with the download locations marked and (b) view of the discs after they have been downloaded

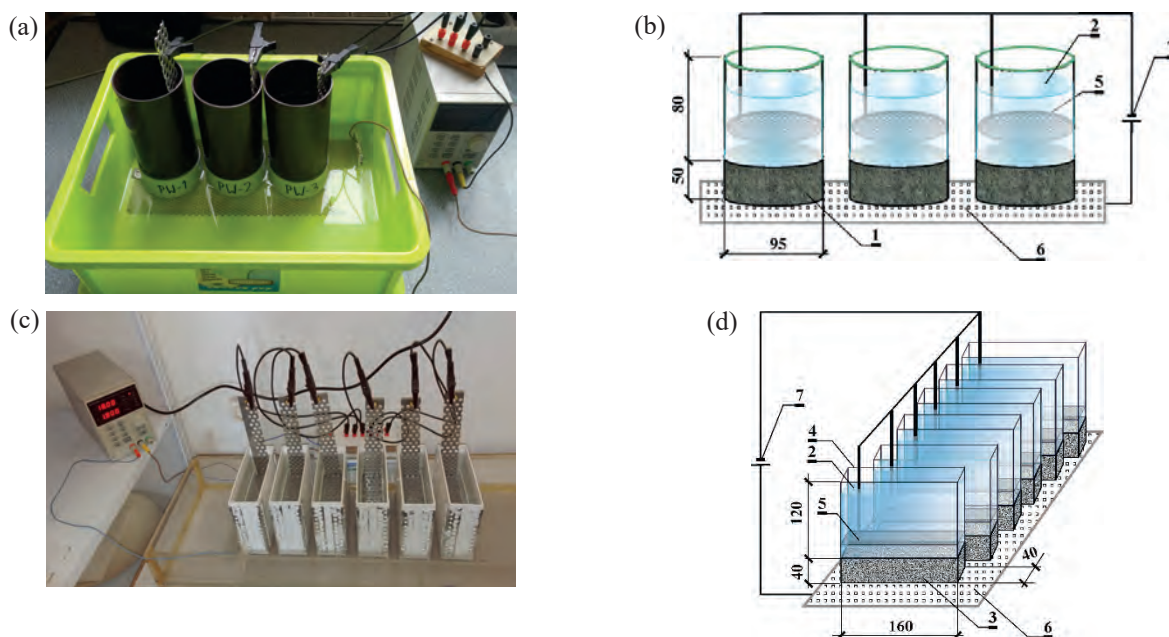


Fig. 3. Chloride migration test stands: a) view of test of cylindrical specimens cut from HC-500 slabs; b) schematic of test of cylindrical specimens cut from HC-500 slabs; c) view of test of lightweight concrete rectangular specimens; d) schematic of test of lightweight concrete rectangular specimens – description in text

After migration, the samples were left under laboratory conditions for 3 days. Then some of the samples were subjected to strength tests. In the remaining samples, the level of chloride ion concentration in the aqueous extract was determined using a multifunction meter CX-701 from Elmetron. This extract was obtained, from stratified ground concrete taken with the Profile Grinding Kit device, from layers 4 mm thick to a depth of 40 mm [9]. Table 3 summarizes the designations and dimensions of the samples, along with the tests to which they were subjected.

Strength tests of rectangular specimens were performed in accordance with PN-EN 196-1 [8] using a PILOT Controls Model 65-L27C12 device. The specimens were subjected to a load until the specimen broke. The bending strength of the rectangular specimens was calculated according to the formula:

$$R_t = \frac{1.5 \cdot F_t \cdot l}{b^3} \quad (1)$$

where:

$R_t$  – flexural strength MPa,

$b$  – lateral length of the beam cross-section, mm,

$F_t$  – breaking load in the middle of the beam, N,

$l$  – distance between supports, mm.

The part of the PILOT Controls Model 65-L27C12 responsible for compressive strength testing provided a load increment speed of 2400 ( $\pm 200$ ) N/s. The device indicated  $F_c$  – the value of the pressure reached when the barrel was crushed. The test was performed on halves of the beams. The prepared pieces were placed laterally on the center of the plate, with the accuracy of the  $\pm 0.5$  mm in the longitudinal direction, so that the faces of the beam protruded about 10 mm beyond the plates. Throughout the test, the load was increased uniformly at a rate of 2400 N/s until crushing. The compressive strength was calculated according to the formula:

$$R_c = \frac{F_c}{1600} \quad (2)$$

In order to determine the tensile strength of cylindrical specimens, the indirect method of determining the tensile strength of brittle materials, the Brazilian method, was used, by compressing the cylinder on the side with two linear equivalent loads [10]. The test was performed using a specialized hydraulic press FORM+TEST Prufsysteme Model MEGA 3-3000-100 S – Figure 4.

The splitting tensile strength (Brazilian method) was calculated according to the formula:

$$f_t = \frac{2 \cdot P_{\max}}{\pi \cdot d \cdot h} \quad (3)$$

where:

$f_t$  – splitting tensile strength MPa,

$P_{\max}$  – destructive force on the sample kN,

$d$  – sample diameter, mm,

$h$  – sample height, mm.

Testing of the modulus of elasticity of lightweight concrete beams was carried out using the guidelines provided in the ITB manual 194:98 [11]. All samples were divided into two equal halves (to reduce slenderness), and one of each was selected for further analysis. In order to measure deformation, two paper strain gauges, 20 mm each, were taped the samples, on opposite sides of the longitudinal beams. The test was performed using a specialized hydraulic press FORM+TEST Prufsysteme Model MEGA 3-3000-100 S.

Simultaneously, the pressure of the applied force and strain were checked for both strain gauges at a frequency of 0.5 s intervals. The pressure increment was 0.1 kN/s. The specimens were positioned axially in the testing press and loaded with an initial force, inducing a stress of  $\sigma = 0.5$  MPa in the specimen. The press then increased the pressure on the specimen until it failed. The strain values were automatically measured and entered into a computer connected to the test press. Calculations of the modulus of elasticity for individual specimens were made using the formula:

$$E_{cmi} = \frac{\Delta \sigma}{\Delta \varepsilon} \quad (4)$$

where:

$E_{cmi}$  – modulus of elasticity, MPa,

$\Delta \sigma$  – the difference in stress in the specimen between the stress corresponding to the initial load and the stress corresponding to the load with a value of  $0.4f_{cm}$ , MPa,

$\Delta \varepsilon$  – the difference in the deformation of the specimen between the initial load and the final load with a value of  $0.4f_{cm}$ , %.

### 3. RESULTS AND DISCUSSION

Table 4 shows the results of chloride ion concentrations determined in cylindrical samples cut directly from HC-500 slabs and samples made from lightweight concrete after accelerated penetration of chloride ions into the concrete. A higher value of chloride ion concentration obtained in cuboidal samples made of lightweight concrete was observed, compared to samples taken directly from HC-500 slabs, which results from the

Table 3. Distribution of chloride ion concentration values determined in cylindrical samples cut from HC-500 slabs and beams made from lightweight concrete

Rzędna obl./ Coordinate [mm]	Cl <sup>-</sup> concentration in c <sup>1</sup> Solution [mg/dm <sup>3</sup> ]	Chloride content by cement mass [%]	Cl <sup>-</sup> concentration in c <sup>1</sup> solution [mg/dm <sup>3</sup> ]	Chloride content by cement mass [%]
<b>Concrete</b>	<b>Concrete in HC-500 slabs</b>		<b>Leight weight concrete</b>	
2	246.8	0.270	699	0.20
6	45.9	0.05	152.1	0.043
10	20.1	0.023	74.6	0.021
14	17.1	0.019	51.3	0.015
18	16.1	0.018	46	0.013
22	15.8	0.017	37.5	0.011
26	15.4	0.017	31.2	0.009
30	15.6	0.017	27.3	0.008
34	15.0	0.016	22.3	0.006
38	14.9	0.016	18.9	0.005

more compact structure of cylindrical samples. After converting the chloride ion content expressed as a percentage by weight of cement, the concentration distribution obtained in cylindrical samples was slightly greater up to a depth of 10 mm. In contrast, as the depth increased, the predominance of chloride content in concrete cut from HC-500 slabs increased.

Figure 4 shows the results of strength tests on cuboid specimens made of lightweight concrete. It was observed that specimens PP-2-4, subjected to the penetration of chloride ions with the help of an electric field, obtained a lower average flexural strength (about 41% taking into account the arithmetic mean and 52% taking into account the median of the measured values) and at the same time a higher average compressive strength (about 19% taking into account the arithmetic mean and 18% taking into account the median) with respect to control specimens PP-5-7.

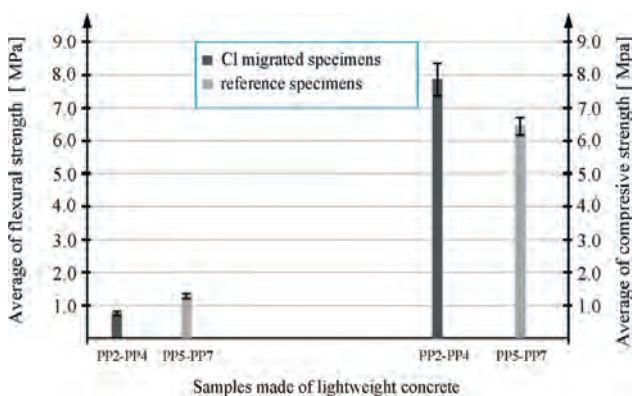


Fig. 4. Graph of average flexural and compressive strength of samples subjected to Cl migration and reference samples made of lightweight concrete

In [12] it was found that specimens cared for in water had higher flexural strength (by 15%) and lower compressive strength than specimens with lower moisture content cared for in a climatic chamber. Concrete in a moist state showed higher tensile strength than dry one, since water in the form of films on colloidal particles causes them to be bonded together more strongly [12]. The salt content of concrete, due to its hydrophilic properties, can bind water, causing it to “dry out” and loosen those bonds, entailing a reduction in flexural strength.

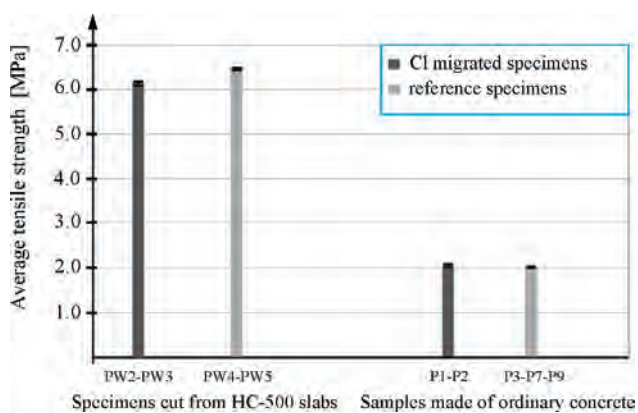


Fig. 5. Graph of average tensile strength of Cl migrated and reference specimens cut from HC-500 slabs and made of ordinary concrete

Figure 5 shows the results of tensile tests (Brazilian method) of cylindrical specimens cut directly from HC-500 slabs (PW-2, PW-3 treated with chloride ions in the process of migration and PW-4, PW-5 without the action of these ions) and cylindrical specimens made from ordinary concrete (P1-P3 made with NaCl

addition and P7, P9 control specimens). It can be seen that in both types of samples the tensile strength almost did not change due to NaCl penetration.

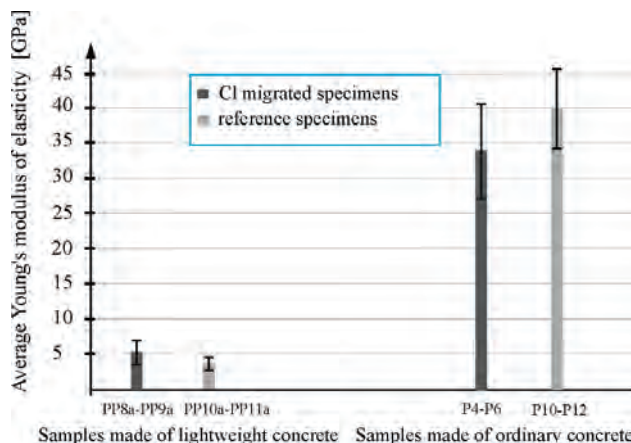


Fig. 6. Graph of average Young's modulus of elasticity of samples subjected to Cl migration and reference samples made of lightweight concrete and ordinary concrete

Figure 6 shows the results of tests on the modulus of elasticity of rectangular specimens made from lightweight concrete and cylindrical specimens prepared from ordinary concrete. It can be observed an increase of about 42% taking into account the arithmetic mean (about 64% taking into account the median) in the value of the modulus of elasticity of PP-8a-9a beams treated with chloride ions with respect to the control specimens PP-10a-11a. However, in the case of cylindrical specimens made of ordinary concrete, a reduction of about 17% taking into account the arithmetic mean (about 20% taking into account the median) in the value of the modulus of elasticity of P4-P6 beams treated with chloride ions can be observed with respect to P10-P12 control specimens. The figure also indicates the variance of the standard deviation calculated for each group of results. The dispersion of the results, as determined by the value of the standard deviation, can be considered average, but each time its value was less than or slightly exceeding 1/3 of the average value of the measured values. Of course, such tests should be carried out on a larger number of samples in order to reduce the dispersion of the values obtained and assess the effects of salinity on concrete.

## REFERENCES

- [1] Amalia Z., Qiao D., Nakamura H., Miura T., and Yamamoto Y., *Development of simulation method of concrete cracking behavior and corrosion products movement due to rebar corrosion*, Constr. Build. Mater., vol. 190, pp. 560–572, 2018, doi: 10.1016/j.conbuildmat.2018.09.100.
- [2] Fyall Z., Wysocki L., *Korozja lugująca w żelbetowych zbiornikach do magazynowania wody przeznaczonej do spożycia*, Mater. Bud., vol. 1, no. 2, pp. 29–32, 2022, doi: 10.15199/33.2022.02.07.

## 4. CONCLUSIONS

Based on the conducted preliminary studies of the mechanical properties of various types of concrete, it can be concluded that:

- The flexural strength of lightweight concrete decreased about 41% taking into account the arithmetic mean and 52% taking into account the median of the measured values due to the addition of salt, in contrast to the compressive strength, which increased by about 19% taking into account the arithmetic mean and 18% taking into account the median. The flexural strength of the concrete is more sensitive to the salt content than the compressive strength, which may be related to a decrease in the moisture content of the tested concrete due to the hydrophilic properties of salt.
  - Using the Brazilian method to evaluate the effect of salt content both added directly to the concrete mix and introduced by the migration method showed no change in tensile strength, similar to what was found in the [7].
  - Tests of the modulus of elasticity of ordinary concrete indicate a slight decrease (about 17% taking into account the arithmetic mean (about 20% taking into account the median) in Young's modulus associated with the addition of chlorides directly to the concrete mix.
  - On the other hand, a definite increase about 42% taking into account the arithmetic mean (about 64% taking into account the median) in the value of elastic modulus was obtained in lightweight concrete in samples treated with chloride ions in an electric field, which confirms the dependence of elastic modulus on compressive strength contained in the standard [13].
- The findings suggest the importance of conducting additional research on the mechanical properties of various types of concrete, including the study of microstructure and chemical composition, in particular, the content of Ca/Si and the amount of calcium hydroxide. Such studies would allow for more accurate modelling of concrete cracking under corrosive conditions induced by chloride ions, examining both the variations in the volume of reinforcement corrosion products and the changes in the mechanical properties of chloride-contaminated concrete.



- [3] Shi et al. Z., *Role of calcium on chloride binding in hydrated Portland cement–metakaolin–limestone blends*, *Cem. Concr. Res.*, vol. 95, pp. 205–216, 2017, doi: 10.1016/j.cemconres.2017.02.003.
- [4] Guru Jawahar J., Sashidhar C., Ramana Reddy I.V., Annie Peter J., *Micro and macrolevel properties of fly ash blended self compacting concrete*, *Mater. Des.*, vol. 46, pp. 696–705, 2013, doi: 10.1016/j.matdes.2012.11.027.
- [5] Jain S., Pradhan B., *Fresh, mechanical, and corrosion performance of self-compacting concrete in the presence of chloride ions*, *Constr. Build. Mater.*, vol. 247, p. 118517, 2020, doi: 10.1016/j.conbuildmat.2020.118517.
- [6] Park S.S., Kwon S.J., Song H.W., *Analysis technique for restrained shrinkage of concrete containing chlorides*, *Mater. Struct. Constr.*, vol. 44, no. 2, pp. 475–486, 2011, doi: 10.1617/s11527-010-9642-4.
- [7] Miarka P. et al., *Influence of chlorides on the fracture toughness and fracture resistance under the mixed mode I/II of high-performance concrete*, *Theor. Appl. Fract. Mech.*, vol. 110, pp. 1–25, 2020, doi: 10.1016/j.tafmec.2020.102812.
- [8] 196-1:2016 PN-EN, “Metody badania cementu. Część 1: Oznaczenie wytrzymałości.; Polish Committee for Standardization”.
- [9] Perkowski Z., Szweda Z., *The ‘Skin Effect’ Assessment of Chloride Ingress into Concrete Based on the Identification of Effective and Apparent Diffusivity*, *Appl. Sci.*, vol. 12, no. 3, pp. 2–25, 2022, doi: 10.3390/app12031730.
- [10] Podgórski J., Gontarz J., *Wyznaczenie wytrzymałości na rozciąganie betonu i skał metodą ‘brazylijską’ w konfrontacji z zastosowanym kryterium zniszczenia materiału*, *Bud. i Architekt.*, vol. 13, no. 2, pp. 191–200, 2014.
- [11] Nr 194/98 ITB, “Badania cech mechanicznych betonu na próbkach wykonanych w formach, Instytut Techniki Budowlanej, Warszawa, 1998”.
- [12] Konopska-Piechurska M., Jackiewicz-Rek W., *Czynniki decydujące o właściwościach wytrzymałościowych betonu do nawierzchni*, *Budownictwo, Technologie, Architektura*, vol. 1; ISSN: 1, pp. 48–52, 2016.
- [13] PN-EN 1992-1-1. *Projektowanie konstrukcji z betonu: Reguły ogólne i reguły dla budynków*. Polski Komitet Normalizacyjny, pp. 1–2, 2016.

#### **Formatting of funding sources**

*This research did not receive any specific grants from funding agencies in the public, commercial, or not-for-profit sectors.*



# A NEW APPROACH TO THE ACCELERATED METHOD FOR ASSESSING THE ALKALI REACTIVITY OF DOMESTIC AGGREGATES

## NOWE PODEJŚCIE DO PRZYSPIESZONEJ METODY BADANIA REAKTYWNOŚCI ALKALICZNEJ KRUSZYW KRAJOWYCH

Justyna Zapała-Sławeta,  
Kielce University of Technology, Poland

Kamil Zięba\*,  
Kielce University of Technology, Poland  
Centrum Technologiczne Betotech sp. z o.o., Dąbrowa Górnicza, Poland

### Abstract

*In Poland, the prevailing protocols for examining the alkali reactivity of aggregates are based on indirect methodologies such as petrographic appraisal, in addition to direct methodologies including the measurement of expansion in mortar and concrete specimens containing the aggregate under investigation. The available research methods exhibit certain deficiencies, which have been mitigated under the experimental conditions delineated in the novel accelerated approach for ascertaining the reactivity of aggregates, otherwise known as the MCPT – Miniature Concrete Prism Test. The methodology of MCPT has the potential to become an alternative for the existing procedures of quality assessment for both fine and coarse aggregates. This work presents the assessment results of the alkaline reactivity of indigenous fine quartz aggregate, examined in accordance with the protocols established by the Polish General Directorate for National Roads and Motorways along together the novel, expedited MCPT methodology.*

**Keywords:** alkali-aggregate reaction, testing methods, mcpt method, correlation

### Streszczenie

*Obecnie stosowane w Polsce procedury badania reaktywności alkalicznej kruszyw oparte są na metodach pośrednich, takich jak ocena petrograficzna oraz metodach bezpośrednich, polegających na określaniu ekspansji próbek zapraw i betonów z badanym kruszywem. Dostępne metody badawcze wykazują pewne wady, które zostały ograniczone w warunkach badawczych ustalonych w nowej przyspieszonej metodzie określania reaktywności kruszyw, tzw. MCPT – Miniature Concrete Prism Test. Metoda MCPT może stać się alternatywą dla obecnego testowania jakości kruszyw drobnych i grubych. W pracy przedstawiono wyniki oceny reaktywności alkalicznej krajowego drobnego kruszywa kwarcowego, badanego zgodnie z procedurami Generalnej Dyrekcji Dróg Krajowych i Autostrad oraz nowej przyspieszonej metody MCPT.*

**Słowa kluczowe:** korozja alkaliczna kruszywa, metody badawcze, metoda MCPT, korelacja

### 1. INTRODUCTION

The reaction of sodium and potassium hydroxides found in the pore fluid of concrete with specific types of aggregate silica (ASR) results in a reduction in the

durability of the concrete, and, in severe instances, leads to its complete disintegration. The reaction yields a hygroscopic gel of sodium and potassium silicates, containing calcium ions and exhibiting

\*Kielce University of Technology, Poland, e-mail: [kamil.zieba@heidelmbergmaterials.com](mailto:kamil.zieba@heidelmbergmaterials.com)

expansion capabilities [1]. The implications of ASR, such as failures of civil engineering structures, the lack of ability or extensive costs of building repairs, render the assessment of the quality of aggregates used in concrete as a current and crucial matter in modern concrete technology.

The main method of preventing ASR-induced concrete damage is the use of aggregates that which are environmentally compatible. For this purpose, appropriate classification of aggregates is required, as it allows for potential additional limitations in the concrete mixture. Research methods for evaluating the reactivity of aggregates have been a focus of extensive, worldwide, and their development has been continuously ongoing since the 1940s [2].

The technical directives of the Polish General Directorate for National Roads and Motorways to establish the appropriateness of aggregate for application in structural concrete necessitate conducting a petrographic assessment (in accordance with PB/3/18 [3]) which considers the detection of reactive silica forms in the aggregate [4]. The classification of aggregate reactivity, which includes non-reactive (R0), moderately reactive (R1), highly reactive (R2), and extremely reactive (R3), is determined through direct methods by evaluating the elongation rate of mortar and concrete specimens. The accelerated testing method in accordance with procedure PB/1/18 [5], based on the guidelines issued by ASTM C1260 [6] and RILEM AAR-2 [7], allow for a fast assessment of the reactivity degree of aggregate based on measuring linear changes in the elongation of cement mortars stored for 14 days in a 1M NaOH solution at 80°C [5]. The harsh conditions of the research methodology, coupled with the necessity for mechanical fragmentation of coarse aggregates into requisite fractions for analysis, frequently lead to erroneous classification. In light of the considerable number of false positives and the relatively small number of false negatives, many researchers consider the faster method to be a reliable means of determining the absence of damaging reactivity in an aggregate [8, 9]. The study is particularly advantageous for aggregates that exhibit a low rate of reaction [10].

The research method that most closely approximates actual conditions is that outlined in the PB/2/18 procedure [11], which is based on the methods set forth in the ASTM C1293 [12] and RILEM AAR-3 [13] standards. The concrete specimens are maintained at a temperature of 38°C and a relative

humidity exceeding 95% for a period of 12 months. Although the method is considered to be dependable, the one-year assessment period makes it unsuitable for continuous monitoring of aggregate quality. A further limitation of the long-term method is the considerable degree of alkali leachability, which may lead to an underestimation of the expansion results of the tested specimens. It has been demonstrated that approximately 35% of the original alkalis present in the concrete samples examined are leached over the course of a year, with approximately 20% being leached after just 90 days. These findings are supported by the literature, with sources [14-16] providing similar evidence.

The weak correlation between the results of mortar expansion and the expansion of concretes with aggregates of varying reactivity, investigated by accelerated and long-term methods, prompted the development of a new research method, MCPT, by Latifee and Rangaraju [17]. This novel approach to the study of fine and coarse aggregates represents a modification and adaptation of the methodologies outlined in ASTM C1260 and ASTM C1293. The elevation of the testing temperature from 38°C, as utilised in the ASTM C1293 standard method, to 60°C in the MCPT method has the effect of accelerating the reaction and consequently the expansion of concrete containing reactive aggregate. Nevertheless, the utilisation of an immersion solution (1M NaOH) effectively inhibits the leaching of alkalis from concrete. The MCPT method does not include any stipulations regarding the fragmentation of the tested aggregates for the purpose of adjusting their grain size grading. The investigation period has been protracted from 56 days to 84 days for slowly reactive aggregates. A notable correlation exists between the results obtained via the MCPT method and those procured through the long-term method (ASTM C1293). Conversely, a weaker correlation is observed between MCPT and the accelerated method (ASTM C1260) for non-reactive, moderately reactive and highly reactive aggregates [18]. Moreover, the MCPT method is regarded as a reliable and precise technique for assessing the reactivity of aggregates and the effectiveness of ASR preventive measures in comparison to the AMBT method, particularly for aggregates with high reactivity [19]. Furthermore, it is essential to confirm a better correlation between the expansion results obtained through MCPT techniques and the outcomes achieved through the long-term method for coarse aggregates in comparison to fine aggregates [17]. The universality

of the new method for evaluating aggregate reactivity necessitates further investigation – currently, the data concerning determining correlations, particularly for slowly reactive or moderately reactive aggregates, still remains insufficient. The objective of the studies presented in the article is to evaluate the reactivity of fine aggregate based on the results of mortar and concrete expansion tests obtained using research methods PB/1/18, PB/2/18, and MCPT. The work was based on an examination of an aggregate containing cryptocrystalline quartz as a reactive component and deformed quartz, which are minerals that are considered to react more slowly with alkalis [20-22].

## 2. MATERIALS AND RESEARCH METHODS

### 2.1. Cement

The mortar and cement samples were prepared using CEM I 52.5R cement with an alkali content expressed as equivalent  $\text{Na}_2\text{O}_{\text{eq}}$  at a level of 0.87%. The chemical composition is delineated in Table 1.

### 2.2. Aggregate

The studies used domestic, medium-grained quartz sand (0/2 mm) with a significant proportion of carbonate lithoclasts. Granite was employed as

the non-reactive coarse aggregate, with fractions of 2/8 mm and 8/16 mm. The findings of the studies conducted in accordance with PB/1/18, PB/2/18 and PB/3/18 substantiate the non-reactive nature of the aggregate. The mineralogical composition of the fine aggregate, together with the determination of the types and percentage share of reactive silica forms, is presented in Table 2 and Figure 1. The petrographic analysis of the aggregate was conducted in accordance with the procedures set forth in guideline PB/3/18 issued by the Polish General Directorate for National Roads and Motorways. The samples under investigation were subject to reduction, following which they were meticulously prepared for observation under the conditions of transmitted light polarisation, as per the guidelines laid out in the PN-EN 12407 standard [23]. The visual inspection of the aggregate material was executed through an Olympus BX-51 polarising microscope. In the course of the research, two lenses were employed: a 5× and a 10× lens. The images were obtained using an Olympus SC180 camera. The planimetric analysis was conducted in a grid with a 0.4 mm pitch, with a total of over 1500 counts.

Table 1. Oxide composition of cement

Cement type	Oxide composition [%]									
	SiO <sub>2</sub>	Al <sub>2</sub> O <sub>3</sub>	Fe <sub>2</sub> O <sub>3</sub>	CaO	MgO	SO <sub>3</sub>	Na <sub>2</sub> O	K <sub>2</sub> O	LOI	Na <sub>2</sub> O <sub>eq</sub>
CEM I 52.5R	19.2	5.05	3.01	64.0	2.1	3.48	0.26	0.92	1.98	0.87

Table 2. The particulate constituents present in the fine-grade aggregate were identified

Component	Description	Percentage rate [%]
Quartz	The lithoclastic constituents were composed of cryptocrystalline and polycrystalline quartz fragments	5
Deformed quartz (with wavy attenuation)	The grains exhibited a range of shapes, ranging from semi-angular to rounded, and a corresponding range of diameters, from 0.1 to 1.6 mm (see Fig. 1)	41
Polycrystalline quartz	Particles with a crystal size <0.010 mm (cryptocrystalline in nature) typically exhibit a well-rounded morphology, frequently culminating in the formation of larger grains with dimensions reaching up to 1 mm (see Fig. 1)	36
Quartz exhibiting homogeneous light attenuation	Well-rounded, with an average diameter of 0.4 mm	10
Feldspar grains	The particles of potassium feldspar are manifested as microcline, Carlsbad law-compliant orthoclase twinning, and perthitic intergrowths. They are exceptionally rounded with markedly smaller dimensions, not exceeding 0.3 mm	9
Lithoclasts	A small number of grains of semi-rounded fragments of metamorphic rocks (such as sericite schists)	7

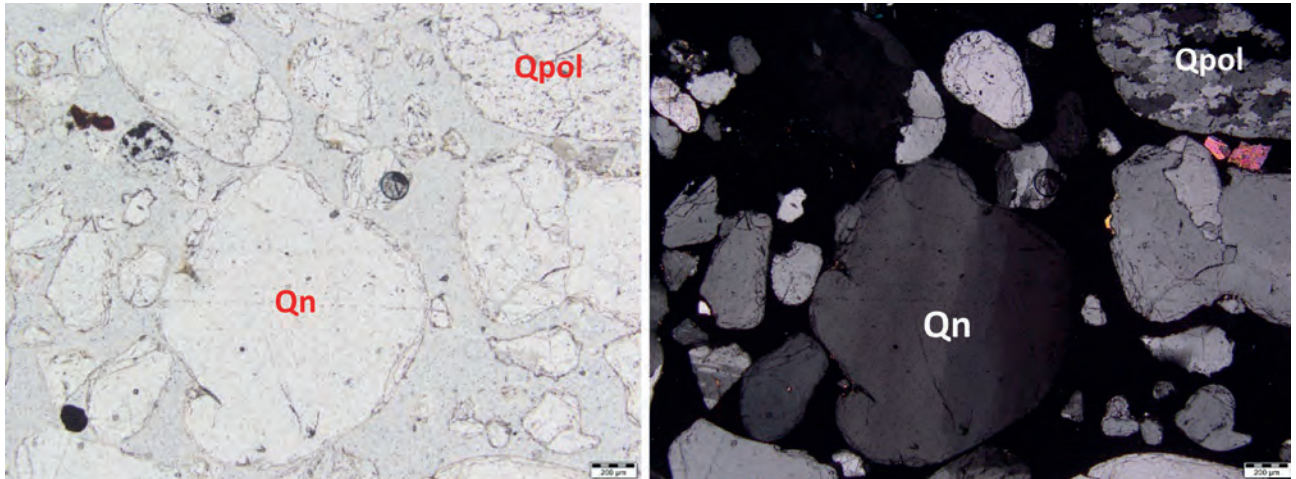


Fig. 1. The sample’s microscopic representation exhibits prominently spherical grains of quartz with wavy attenuation (known as deformed Qn quartz), in conjunction with polycrystalline quartz (Qpol) (refer to figures 1N and XN)

### 2.3. Research procedures

The categorisation of the reactivity of the examined fine aggregate was conducted through the measurement of linear elongation of samples utilising three methodologies: the procedures PB/1/18 and PB/2/18, as well as the modified MCPT method. The modification entailed alterations in the granularity and proportion of individual fractions. The fine aggregate of the 0/4 mm fraction constituted 40% of the total aggregate mass, while the coarse aggregate of the 4/22 mm fraction accounted for 60%. This methodology was developed as a means of calibrating the granulometry of aggregates to align with the standard aggregate blend employed in the PB/2/18 protocol. Table 3 presents a comparison of the employed methods for assessing the potential alkali reactivity of aggregates, along with an indication of the differences in relation to the original MCPT method.

In accordance with the specifications of the MCPT method, three concrete specimens of dimensions 50 × 50 × 285 mm were prepared. The specimens were stored in moulds under conditions of high humidity (relative humidity >95%) for a period of 24 hours, after which they were transferred to water at a temperature of 60°C. Two days following the moulding process, the initial length of the specimens was measured. Thereafter, the concrete bars were placed in a 1M NaOH solution at 60°C. The linear changes of these specimens were measured at intervals of 3, 5, 7, 10, 12, 14, 21, 28, 42, and 56 days using a Graf-Kaufman device.

### 3. RESULTS

The expansion trajectory of mortar and concrete bars utilising the aforementioned fine aggregate is illustrated in Figures 2a-c. The delineation of aggregate reactivity, indicated by red lines,

Table 3. Analysis of methodologies for evaluating potential reactivity of aggregates

Research method	PB/1/18 [5]	PB/2/18 [11]	MCPT [17]	MCPT (modified)
Dimensions of the specimens [mm]	25 x 25 x 285	75 x 75 x 285	50 x 50 x 285	50 x 50 x 285
Dimensions of the aggregates [mm]	0.125 – 4	<22	<12.5	<22
Cement content [kg/m <sup>3</sup> ]	440	420±10	420	420
W/c (water-cement ratio)	0.47	0.42-0.45	0.45	0.45
Increase in Na <sub>2</sub> O <sub>eq</sub> [%] content	None	1.25	1.25	1.25
Storage conditions	1M NaOH, 80°C	RH>95%, 38°C	1M NaOH, 60°C	1M NaOH, 60°C

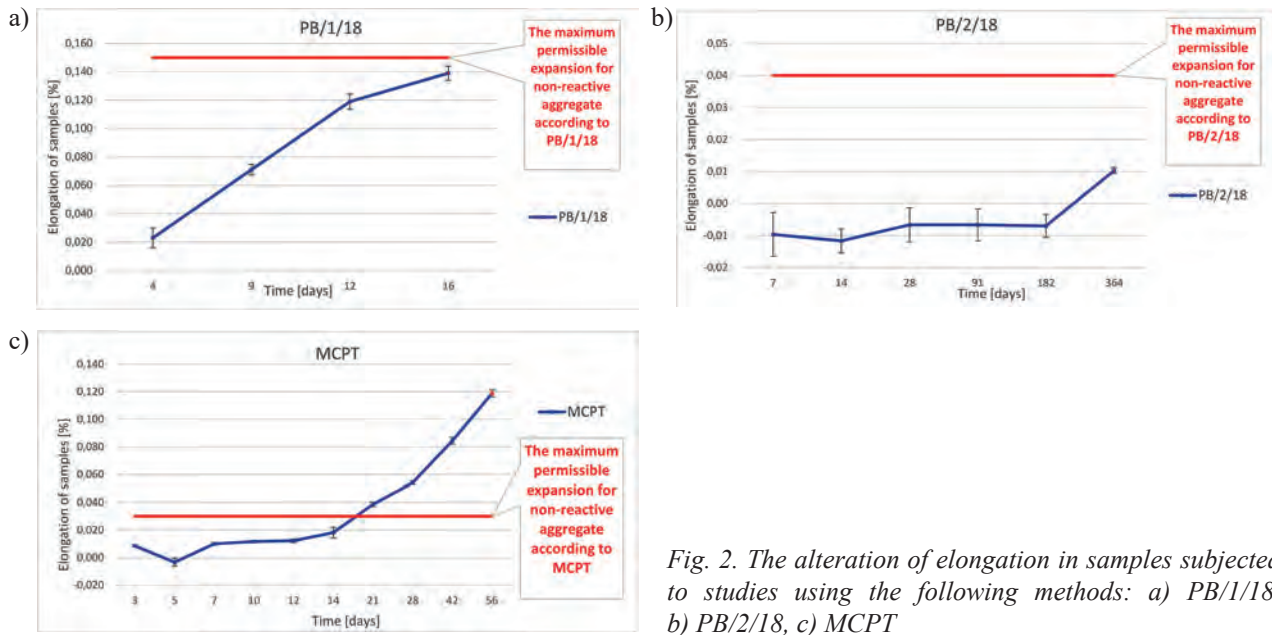


Fig. 2. The alteration of elongation in samples subjected to studies using the following methods: a) PB/1/18, b) PB/2/18, c) MCPT

Table 4. Categorisation of aggregate reactivity for concrete [24]

Research method	PB/1/18 [5]	PB/2/18 [11]	MCPT [17]	MCPT (modified)
Upper limit of expansion	NR: 0.15% after 2 weeks MR: 0.30 after 2 weeks HR: 0.45% after 2 weeks	NR: 0.04% after 52 weeks MR: 0.12% after 52 weeks HR: 0.24% after 52 weeks	NR: 0.03% <sup>1</sup> after 8 weeks SR: 0.04% after 8 weeks MR: 0.12% after 8 weeks HR: 0.24% after 8 weeks	NR: 0.03% after 8 weeks <sup>1</sup> SR: 0.04% after 8 weeks MR: 0.12% after 8 weeks HR: 0.24% after 8 weeks

where: NR – non-reactive aggregate, MR – moderately reactive aggregate, HR – highly reactive aggregate, SR – slowly/weakly reactive aggregate.

<sup>1</sup> or 0.04%, if the expansion rate from 8 to 12 weeks is  $\leq 0.010\% / 2$  weeks

categorises the aforementioned aggregates into distinct classifications in accordance with the data presented in Table 4.

In accordance with the established expansion criteria, the quartz aggregate was categorised as follows:

- non-reactive aggregates according to procedure PB/1/18 issued by the GDDKiA (General Directorate for National Roads and Motorways) due to an expansion value after 14 days  $\leq 0.15$ ;
- non-reactive aggregates according to procedure PB/2/18 issued by the GDDKiA (General Directorate for National Roads and Motorways) due to an expansion value after 365 days  $\leq 0.04$ ;
- aggregates with a medium degree of reactivity, in accordance with the new accelerated MCPT method, due to the expansion value after 56 days  $\leq 0.120$ ;

#### 4. DISCUSSION OF RESULTS

The results of petrographic aggregate examinations indicated the presence of potentially reactive forms of silica, including cryptocrystalline quartz and distorted quartz. Small quartz crystals had dimensions of  $<10\mu\text{m}$ . Scientific literature suggests that the reactivity of specific silica forms is influenced by the extent of structural imperfections and the dimensions of the crystallite grains [21]. The process of reducing the dimensions of quartz grains, which concurrently expands the surface area susceptible to alkali reactions, results in an amplification of the reactive properties of the material. In accordance with the classification outlined in the Norwegian Standards, crystallites with a size of  $<60\mu\text{m}$  are deemed capable of reacting with alkalis, exhibiting high reactivity within the grain size range of  $<10\mu\text{m}$ , and a lesser degree of reactivity within the range of  $10\text{--}60\mu\text{m}$ .

Nonetheless, it is recognised that the reactivity of granules measuring 60-130  $\mu\text{m}$  is uncertain [25]. Furthermore, it has been established that the quartz content within the boundary layer with a grain size of 10  $\mu\text{m}$ , is approximately 2.6% by volume. However, it is advised to reduce the permissible value to 2% [20]. An investigation of the grains of siliceous aggregate revealed that they contain over 36% of minerals that are capable of reacting with alkalis.

The trajectory of expansion curves ascertained by the three methods being examined exhibits significant deviations between one another. The elongation of samples tested by the accelerated method in accordance with the PB/1/18 procedure demonstrates a uniform increase up to the 12th day of the test. Following a 14-day period, the expansion value reached 0.139%, which is situated close to the lower boundary and thus categorises the aggregate as moderately reactive. In accordance with the aggregate reactivity classification per ASTM C1260, the examined aggregate should be classified as moderately reactive (range  $0.101 \leq X \leq 0.200$ ). The expansion curve for concrete samples tested in accordance with the MCPT method exhibits a distinct trajectory. In the initial period, up to the 12th day, the expansion is observed to increase to a small extent, however after that period, it does amplify. The expansion value of the samples after 56 days is 0.119%, which is similar to the upper limit for classifying the aggregate as moderately reactive (range  $0.041 \leq X \leq 0.120$ ). The values of linear length changes in concrete samples, as determined by the PB/2/18 procedure, indicate the occurrence of concrete shrinkage up to the 180<sup>th</sup> day. The final value of the concrete sample expansion, i.e., after 360 days, is 0.01%, which is markedly lower than the threshold value for aggregate classification as moderately reactive ( $X > 0.04$ ). It must be noted that an elevated test temperature and the provision of an external source of alkalis facilitate the acceleration of the reaction between the examined quartz sand and alkalis. The elongation of the concrete bars was examined according to the methodology specified in procedure PB/2/18, thus under conditions most closely corresponding to real conditions, which indicates the absence of a harmful aggregate reaction with alkalis. The observed increase in expansion at a later time may be indicative of a delayed reaction of deformed quartz forms that are contained within the aggregate. Moreover, the elevated test temperature and the availability of an external NaOH source in the MCPT method provide an environment conducive to the reaction of silica with alkalis, in comparison to the

conditions of the long-term method. The more lenient conditions specified in procedure PB/2/18, when considered alongside the potential for increased alkali leaching from concrete samples, may ultimately result in a reduction in the values of measurable concrete expansion [18].

## 5. CONCLUSIONS

The findings of the study have enabled to formulate the following conclusions:

1. The examined siliceous aggregate was found to contain potentially reactive forms of silica, including cryptocrystalline quartz with grains measuring less than 10  $\mu\text{m}$  and deformed quartz.
2. The investigative techniques for aggregate reactivity, in compliance with PB/1/18, PB/2/18 and MCPT, denote a disparity in the sensitivity of the aggregate towards the alkali – silica reaction. The linear elongation values obtained for concrete samples were used to classify the fine aggregate as moderately reactive in accordance with the MCPT method. However, the results of tests conducted in accordance with the PB/1/18, and PB/2/18 procedures indicated the absence of a harmful aggregate reaction with alkalis.
3. The results of the expansion studies conducted in accordance with the procedures specified in PB/1/18 and PB/2/18 categorise the fine aggregate into various reactivity categories, rendering it suitable for use in R1 and R0. The recorded final values of expansion obtained through the MCPT and PB/1/18 methods are found to be similar. Following an analysis of the findings from the Miniature Concrete Prism Test, the aggregate was categorised as belonging to the SR grouping, which denotes a slow and weak reactivity.
4. The parameters of the reaction such as temperature, humidity, presence of antagonistic ions in relation to silica, and the period of investigation, exert an impact on the progression of corrosive processes.
5. The study results demonstrate the necessity for further enhancement of the existing methodologies for the determination of alkali reactivity of aggregates in Poland. The proposal of an alternative method for examining concrete sample expansion (MCPT – Miniature Concrete Prism Test) represents a potential avenue for improvement, addressing some of the shortcomings of the current procedures. However, further research is required to confirm the effectiveness and accuracy of this proposed method.

**REFERENCES**

- [1] Poole A.B.: *Introduction to Alkali – Aggregate Reaction in Concrete*. Materials Science Engineering, 1991, DOI:10.4324/9780203036631-3.
- [2] Stanton T.E.: *Expansion of Concrete Through Reaction Between Cement and Aggregate*. Proc. American Society of Civil Engineers, 66(10), 1941, pp. 1781–1811.
- [3] Giergiczny Z., Machniak Ł., Golda A., Witczak S., Adamski G., Bukowski L., Szewczyk E., Nowek M., Brykalski W.: *Appendix 1 of the Technical Guidelines for the Classification of Domestic Aggregates and Prevention of the Alkali-Aggregate Reaction in Concrete Road Pavements and Road Engineering Facilities*, Part II, Test Procedure PB/3/18. General Directorate for National Roads and Motorways, 2022.
- [4] Giergiczny Z., Machniak Ł., Golda A., Witczak S., Adamski G., Bukowski L., Szewczyk E., Nowek M., Brykalski W.: *Wytyczne techniczne klasyfikacji kruszyw krajowych i zapobiegania reakcji alkalicznej w betonie stosowanym w nawierzchniach dróg i drogowych obiektach inżynierskich*, Część I. Generalna Dyrekcja Dróg Krajowych i Autostrad, 2022.
- [5] Giergiczny Z., Machniak Ł., Golda A., Witczak S., Adamski G., Bukowski L., Szewczyk E., Nowek M., Brykalski W.: *Appendix 1 of the Technical Guidelines for the Classification of Domestic Aggregates and Prevention of the Alkali-Aggregate Reaction in Concrete Road Pavements and Road Engineering Facilities*, Part II, Test Procedure PB/1/18. General Directorate for National Roads and Motorways, 2022.
- [6] ASTM C1260: Standard Test Method for Potential Alkali Reactivity of Aggregates (Mortar-Bar Method), p. 5.
- [7] RILEM Recommended Test Method AAR-2: Ultra-Accelerated Mortar-Bar Testing. Materials and Structures, 33, 2000, pp. 283–289.
- [8] Tanesi J., Drimalas T., Chopperla K.S.T., Beyene M., Ideker J.H., Kim H., Montanari L., Ardani A.: *Divergence Between Performance in the Field and Laboratory Test Results for Alkali-Silica Reaction*. Transportation Research Record, 2674, 2020, s. 120–134. <https://doi.org/10.1177/03611981209132>.
- [9] Thomas M., Fournier B., Folliard K., Ideker J., Shehata M.: *Test Methods for Evaluating Preventive Measures for Controlling Expansion Due to Alkali-Silica Reaction in Concrete*. Cement and Concrete Research, 36(10), 2006, pp. 1842–1856. <https://doi.org/10.1016/j.cemconres.2006.01.014>.
- [10] Deifalla A.F.: *Potential of Alkali-Silica Reactivity of Unexplored Local Aggregates as per ASTM C1260*. Materials, 15(19), 2022, 6627. <https://doi.org/10.3390/ma15196627>.
- [11] Giergiczny Z., Machniak Ł., Golda A., Witczak S., Adamski G., Bukowski L., Szewczyk E., Nowek M., Brykalski W.: *Appendix 1 of the Technical Guidelines for the Classification of Domestic Aggregates and Prevention of the Alkali-Aggregate Reaction in Concrete Road Pavements and Road Engineering Facilities*, Part II, Test Procedure PB/2/18. General Directorate for National Roads and Motorways, 2022.
- [12] ASTM C1293: Standard Test Method for Determination of Length Change of Concrete Due to Alkali-Silica Reaction, p. 7.
- [13] RILEM Recommended Test Method AAR-3: Detection of Potential Alkali-Reactivity of Aggregates – Method for Aggregate Combinations Using Concrete Prism. Materials and Structures, 33, 2000, pp. 290–293.
- [14] Thomas M.D.A., Fournier B., Folliard K.J.: *Selecting Measures to Prevent Deleterious Alkali-Silica Reaction in Concrete: Rationale for the AASHTO PP65 Prescriptive Approach*. United States. Federal Highway Administration, 2012.
- [15] Rivard P., Bérubé M.A., Ollivier J.P., Ballivy G.: *Decrease of Pore Solution Alkalinity in Concrete Tested for Alkali-Silica Reaction*. Materials and Structures, 40, 2007, pp. 909–921.
- [16] Rivard P., Bérubé M.-A., Ollivier J.-P., Ballivy G.: *Alkali Mass Balance During the Accelerated Concrete Prism Test for Alkali-Aggregate Reactivity*. Cement and Concrete Research, 33, 2003, pp. 1147–1153.
- [17] Latifee P.R., Rangaraju P.: *Miniature Concrete Prism Test: Rapid Test Method for Evaluating Alkali-Silica Reactivity of Aggregates*. Journal of Materials in Civil Engineering, 27, 2015, pp. 4014215.
- [18] Rangaraju P.R., Afshinnia K., Enugula S.S.R., Latifee E.R.: *Evaluation of Alkali-Silica Reaction Potential of Marginal Aggregates Using Miniature Concrete Prism Test (MCPT)*. 15th International Conference on Alkali-Aggregate Reaction, São Paulo, Brazil, 2020.
- [19] Tanesi J., Drimalas T., Chopperla K.S.T., Beyene M., Ideker J.H., Kim H., Montanari L., Ardani A.: *Divergence Between Performance in the Field and Laboratory Test Results for Alkali-Silica Reaction*. Transportation Research Record, Vol. 2674, 2020, s. 1–15. <https://doi.org/10.1177/03611981209132>.
- [20] Broekmans M.A.T.M.: *Structural Properties of Quartz and Their Potential Role for ASR*. Materials Characterization, 53(2-4), 2004, pp. 129–140. <https://doi.org/10.1016/j.matchar.2004.08.010>.
- [21] Antolik A., Józwiak-Niedźwiedzka D.: *Assessment of the Alkali-Silica Reactivity Potential in Granitic Rocks*. Construction and Building Materials, 295, 2021, 123690.



- [22] Zapła-Sławeta J.: *The Use of Computed Tomography and Scanning Microscopy Methods for Assessing the Alkaline Reactivity of Aggregate*. Bulletin of the Polish Academy of Sciences Technical Sciences, 72(3), 2024, e149814. DOI: 10.24425/bpasts.2024.149814.
- [23] PN-EN 12407:2010: Metody Badań Kamienia Naturalnego – Badania Petrograficzne.
- [24] Dziejczak K., Glinicki M.A.: *Risk Assessment of Reactive Local Sand Use in Aggregate Mixtures for Structural Concrete*. Construction and Building Materials, 408, 2023, 133826. <https://doi.org/10.1016/j.conbuildmat.2023.133826>.
- [25] Alaejos P., Lanza V.: *Influence of Equivalent Reactive Quartz Content on Expansion Due to Alkali-Silica Reaction*. Cement and Concrete Research, 42, 2012, pp. 99–104.

*This paper was supported by the Ministry of Education and Science [Doktorat Wdrożeniowy 2023].*



**THE IMPACT OF RECYCLED FINE AGGREGATE  
ON SELECTED PROPERTIES OF CONCRETE**

**WPŁYW DROBNEGO KRUSZYWA Z RECYKLINGU  
NA WYBRANE WŁAŚCIWOŚCI BETONU**

Maja Kępnia, Justyna Pskowska, Aleksandra Garus  
Warsaw University of Technology, Poland

Michał Drabczyk, Sebastian Kasper  
Holcim Polska S.A.

*Structure and Environment* vol. 16, No. 3/2024, p. 129

DOI: 10.30540/sac-2024-011

**Abstract**

*The use of recycled fine aggregate in the production of concrete mixes is one of the elements of a circular economy. However, it is important to ensure that such a modification does not significantly affect the durability of the produced concrete elements. One possible criterion to check whether this condition is met is the practical application of the concept of equivalent concrete properties. The presented studies analyzed the properties of concrete with multi-component cement CEM V/A (S-V) and with recycled fine aggregate. The conducted analyses of the research results showed that with a 15% replacement level of natural sand with recycled sand, it is possible to maintain durability characteristics compared to concrete using only natural sand.*

**Streszczenie**

*Stosowanie drobnego kruszywa z recyklingu do produkcji mieszanek betonowych jest jednym z elementów gospodarki w obiegu zamkniętym. Należy jednak zwrócić uwagę, aby taka modyfikacja nie wpłynęła znacząco na trwałość wykonywanych elementów betonowych. Jednym z możliwych kryteriów jest sprawdzenie, czy warunek ten jest spełniony, jest zastosowanie w praktyce koncepcji równoważnych właściwości betonu. W przedstawionych badaniach analizowano właściwości betonu z cementem wieloskładnikowym CEM V/A (S-V) oraz z drobnym kruszywem z recyklingu. Przeprowadzone analizy wyników badań wykazały, że przy 15% stopniu zastąpienia piasku naturalnego piaskiem z recyklingu możliwe jest zachowanie cech związanych z trwałością w stosunku do betonu z użyciem wyłącznie piasku naturalnego.*

**RESISTANCE OF LOW-EMISSION GEOPOLYMER BINDERS  
WITH FIBERS TO AGGRESSIVE EXTERNAL FACTORS**

**ODPORNOŚĆ NISKOEMISYJNYCH SPOIW GEOPOLIMEROWYCH Z WŁÓKNAMI  
NA DZIAŁANIE AGRESYWNYCH CZYNNIKÓW ZEWNĘTRZNYCH**

Michał Łach, Agnieszka Przybek, Kinga Setlak, Patrycja Bazan, Maria Hebdowska-Krupa  
Cracow University of Technology, Poland

*Structure and Environment vol. 16, No. 3/2024, p. 134*

DOI: 10.30540/sae-2024-012

**Abstract**

*Materials called geopolymers are considered an alternative to common hydraulic binders, but they have certain limitations in many applications due to their brittleness. The use of fibers to reinforce geopolymers can bring the expected results by increasing their compressive strength. This paper presents the results of accelerated durability tests of geopolymers based on coal shale and fly ash reinforced with natural fibers (1% by mass). The results of testing the resistance of such composites to UV radiation, variable temperature cycles and the results of the thermal conductivity coefficient are presented.*

**Streszczenie**

*Materiały zwane geopolimerami uznawane są za alternatywę dla powszechnych spoiw hydraulicznych jednak posiadają one pewne ograniczenia w wielu zastosowaniach ze względu na ich kruchość. Zastosowanie włókien do zbrojenia geopolimerów może przynieść oczekiwane rezultaty zwiększając ich wytrzymałość na zginanie. W niniejszej pracy zaprezentowano wyniki przyspieszonych badań trwałości geopolimerów na bazie łupków węglowych i popiołu lotnego wzmocnionych włóknami naturalnymi (1% mas.). Przedstawiono wyniki badań odporności takich kompozytów na działanie promieniowania UV, zmiennych cykli temperaturowych oraz przedstawiono wyniki badań współczynnika przewodzenia ciepła.*

**ANALYSIS OF THE DEFORMATION OF ROAD SURFACE CONSTRUCTION  
BASED ON MONITORING CLIMATIC FACTORS**

**ANALIZA ODKSZTAŁCENI KONSTRUKCJI NAWIERZCHNI DROGI  
NA PODSTAWIE MONITORINGU CZYNNIKÓW KLIMATYCZNYCH**

Marek Iwański, Grzegorz Mazurek, Przemysław Buczyński  
Kielce University of Technology, Poland

*Structure and Environment vol. 16, No. 3/2024, p. 141*

DOI: 10.30540/sae-2024-013

**Abstract**

*The article presents the results of simulation of the deformation state of a road surface structure intended for traffic categories KR 3-4. Climatic factors such as temperature and humidity were obtained from a database collected based on the installed monitoring. The performed validation of the deformation state indicated a very good fitness of the model to the experimental results, provided that the viscoelastic model. The results indicated that the difference in pavement load time between 1 s and 1200 s in summer may result in an increase in horizontal deformation under the asphalt layer by 949%, and in winter by 74%. The calculated vertical displacement in winter after 1200 seconds of loading is equivalent to the displacement calculated after 1 second of loading the road surface in summer.*

**Streszczenie**

*W artykule przedstawiono wyniki symulacji stanu odkształcenia konstrukcji nawierzchni drogowej przeznaczonej dla kategorii ruchu KR 3-4. Informacje o czynnikach klimatycznych takich jak temperatura oraz wilgotność pozyskano z prowadzonego monitoringu. Wykonana walidacja stanu odkształcenia wskazała na bardzo dobre dopasowanie modelu do wyników eksperymentu pod warunkiem zastosowania modelu lepko-sprężystego. Wyniki symulacji wskazują, że różnica czasu obciążenia nawierzchni pomiędzy 1 s a 1200 s w okresie lata może spowodować wzrost odkształcenia poziomego pod warstwą asfaltową względnie o 94%, natomiast w okresie zimy o 74%. Obliczone przemieszczenie pionowe w okresie zimy po 1200 s trwania obciążenia jest równoważne z przemieszczeniem obliczonym po 1 s obciążenia nawierzchni drogowej w okresie lata.*

**THE IMPACT OF INTERNAL HYDROPHOBIZATION ON THE PROPERTIES  
OF THE CEMENT-BASED MATERIALS WITH MINERAL ADDITIVES**

**WPŁYW HYDROFOBIZACJI OBJĘTOŚCIOWEJ NA WŁAŚCIWOŚCI  
MATERIAŁÓW CEMENTOWYCH Z DODATKAMI MINERALNYMI**

Kalina Materak, Alicja Wieczorek, Marcin Zasada, Marcin Koniorczyk  
Lodz University of Technology, Poland

*Structure and Environment vol. 16, No. 3/2024, p. 148*

DOI: 10.30540/sae-2024-014

**Abstract**

*The paper presents results regarding the possibility and effectiveness of carrying out the internal hydrophobization in cement-based materials with mineral additives such as granulated blast furnace slag, silica dust and silica fly ash. The obtained results indicate that effective internal hydrophobization by using triethoxyoctylsilane is achievable and provides protection against water by decreasing the capillary absorption of water in the material. However, it also affects the hydration process of the binder, which results in a reduction in the compressive strength of the material.*

**Streszczenie**

*W pracy przedstawiono wyniki dotyczące możliwości przeprowadzenia i skuteczności procesu hydrofobizacji objętościowej w materiałach cementowych z dodatkami mineralnymi, takimi jak: granulowany żużel wielkopiecowy, pył krzemionkowy oraz lotny popiół krzemionkowy. Otrzymane wyniki wskazują, że efektywna hydrofobizacja w masie wykonana przy pomocy trietoksyoktylosilanu jest osiągalna i zapewnia ochronę przed działaniem wody w postaci ograniczenia absorpcji kapilarnej w materiale. Jednakże wiąże się ona również z wpływem na proces hydratacji spoiwa, co skutkuje obniżeniem wytrzymałości na ściskanie materiału.*

**ASSESSMENT OF AGGREGATE MIXTURE REACTIVITY  
IN CONCRETE AT 60°C**

**OCENA REAKTYWNOŚCI MIESZANINY KRUSZYW W BETONIE  
W TEMPERATURZE 60°C**

Kinga Dziedzic, Michał A. Glinicki  
Institute of Fundamental Technological Research,  
Polish Academy of Sciences, Warsaw, Poland

*Structure and Environment vol. 16, No. 3/2024, p. 153*

DOI: 10.30540/sae-2024-015

**Abstract**

*Research on the durability of structural concrete requires careful selection of aggregates, particularly considering their reactivity to alkali-silica reaction (ASR). The Miniature Concrete Prism Test (MCPT) allows for shortened testing time and eliminates the need for aggregate crushing, making it a practical alternative to other methods. The aim of the research is to evaluate the reactivity of aggregate mixtures with varying mineral compositions. Research results confirm the significant impact of fine aggregates on concrete expansion in the MCPT method in NaOH solution at 60°C. The observed expansion correlates with a reduction in concrete's elastic modulus.*

**Streszczenie**

*Badania nad trwałością betonu konstrukcyjnego wymagają starannej selekcji kruszyw, szczególnie uwzględniającej ich reaktywność na reakcję alkalia-krzemionka (ASR). Metoda Miniature Concrete Prism Test (MCPT) pozwala na skrócenie czasu badania i eliminację konieczności rozdrabniania kruszywa, co czyni ją praktyczną alternatywą dla innych metod. Celem badań jest ocena reaktywności mieszaniny kruszyw o zróżnicowanym składzie mineralnym. Wyniki badań potwierdzają znaczący wpływ kruszywa drobnego na ekspansję betonu w metodzie MCPT w roztworze NaOH w temp. 60°C. Obserwowana ekspansja koreluje z redukcją modułu sprężystości betonu.*

**THE INFLUENCE OF CHLORIDE IONS CONTENT  
ON THE MECHANICAL PROPERTIES OF CONCRETE**

**WPŁYW ZAWARTOŚCI JONÓW CHLORKOWYCH  
NA WŁAŚCIWOŚCI MECHANICZNE BETONU**

Zofia Szweda  
Silesian University of Technology, Poland

*Structure and Environment* vol. 16, No. 3/2024, p. 158

DOI: 10.30540/sae-2024-016

**Abstract**

*This paper presents an analysis of the effect of concrete salinity on the splitting tensile strength of specimens taken directly from the HC-500 floor slab and the flexural and compressive strength and the value of the modulus of elasticity of specimens made under laboratory conditions from lightweight concrete and ordinary concrete. The tests were carried out in two variants: in the first, chloride ions were introduced into the concrete by the migration method and in the second, as an additive introduced directly with the batch water. The analysis showed that the additive can affect certain mechanical properties of concrete both favorably and unfavorably. The results indicate that it is important to examine the issue of the influence of salinity on concrete's mechanical properties. This knowledge can be applied to the modeling of damage in reinforced concrete structures resulting from exposure to chloride-rich environments.*

**Streszczenie**

*W niniejszej pracy przedstawiono analizę badań wpływu zasolenia betonu na wytrzymałość na rozciąganie przy rozłupywaniu próbek pobranych bezpośrednio z płyty stropowej HC-500 oraz wpływu zasolenia na wytrzymałość na zginanie i ściskanie oraz na wartość modułu sprężystości próbek wykonanych w warunkach laboratoryjnych z betonu lekkiego i betonu zwykłego. Badania przeprowadzono w dwóch wariantach: w pierwszym po wprowadzeniu jonów chlorkowych do betonu metodą migracyjną w próbkach pobranych z płyt HC-500 i wykonanych z betonu lekkiego i w drugim, jako dodatek wprowadzony bezpośrednio z wodą zarobową w próbkach z betonu zwykłego. Przeprowadzone badania porównawcze różnych betonów z dodatkiem NaCl wykazały, że dodatek ten może wpływać zarówno korzystnie, jak i niekorzystnie na niektóre właściwości mechaniczne betonu. Przeprowadzone badania wskazują, że istotne jest dokładniejsze rozpoznanie zagadnienia wpływu zasolenia betonu na jego właściwości mechaniczne, co może być następnie wykorzystane w procesie modelowania zniszczeń konstrukcji żelbetowych wywołanych oddziaływaniem środowiska zawierającego chlorki.*



**A NEW APPROACH TO THE ACCELERATED METHOD FOR ASSESSING  
THE ALKALI REACTIVITY OF DOMESTIC AGGREGATES**

**NOWE PODEJŚCIE DO PRZYSPIESZONEJ METODY BADANIA  
REAKTYWNOŚCI ALKALICZNEJ KRUSZYW KRAJOWYCH**

Justyna Zapała-Sławeta,  
Kielce University of Technology, Poland

Kamil Zięba,  
Kielce University of Technology, Poland  
Centrum Technologiczne Betotech sp. z o.o., Dąbrowa Górnicza, Poland

*Structure and Environment vol. 16, No. 3/2024, p. 166*

DOI: 10.30540/sae-2024-017

**Abstract**

*In Poland, the prevailing protocols for examining the alkali reactivity of aggregates are based on indirect methodologies such as petrographic appraisal, in addition to direct methodologies including the measurement of expansion in mortar and concrete specimens containing the aggregate under investigation. The available research methods exhibit certain deficiencies, which have been mitigated under the experimental conditions delineated in the novel accelerated approach for ascertaining the reactivity of aggregates, otherwise known as the MCPT – Miniature Concrete Prism Test. The methodology of MCPT has the potential to become an alternative for the existing procedures of quality assessment for both fine and coarse aggregates. This work presents the assessment results of the alkaline reactivity of indigenous fine quartz aggregate, examined in accordance with the protocols established by the Polish General Directorate for National Roads and Motorways along together the novel, expedited MCPT methodology.*

**Streszczenie**

*Obecnie stosowane w Polsce procedury badania reaktywności alkalicznej kruszyw oparte są na metodach pośrednich, takich jak ocena petrograficzna oraz metodach bezpośrednich, polegających na określaniu ekspansji próbek zapraw i betonów z badanym kruszywem. Dostępne metody badawcze wykazują pewne wady, które zostały ograniczone w warunkach badawczych ustalonych w nowej przyspieszonej metodzie określania reaktywności kruszyw, tzw. MCPT – Miniature Concrete Prism Test. Metoda MCPT może stać się alternatywą dla obecnego testowania jakości kruszyw drobnych i grubych. W pracy przedstawiono wyniki oceny reaktywności alkalicznej krajowego drobnego kruszywa kwarcowego, badanego zgodnie z procedurami Generalnej Dyrekcji Dróg Krajowych i Autostrad oraz nowej przyspieszonej metody MCPT.*